Dry Process Fluorination of Uranium Dioxide Using Ammonium Bifluoride

by

Charles Burnett Yeamans

B.S., Chemical Engineering and Nuclear Engineering (2001)

University of California, Berkeley

Submitted to the Department of Nuclear Engineering as One Element of Fulfillment of the Requirements for the Degree of Master of Science in Nuclear Engineering

at the

Massachusetts Institute of Technology

September 2003

Signature of Author:_____
Department of Nuclear Engineering
June 30, 2003

Certified by:_____
Kenneth R. Czerwinski
Associate Professor of Nuclear Engineering
Thesis Supervisor

Certified by:_____
John R. FitzPatrick
Technical Staff Member, Lawrence Livermore National Laboratory
Thesis Reader

Accepted by:_____
Jeffery Coderre
Chair, Department Committee on Graduate Studies

THIS PAGE INTENTIONALLY LEFT BLANK

Dry Process Fluorination of Uranium Oxides using Ammonium Bifluoride

by

Charles Burnett Yeamans

Submitted to the Department of Nuclear Engineering as Partial Fulfillment of the Requirements for the Degree of Master of Science in Nuclear Engineering

ABSTRACT

An experimental study was conducted to determine the practicality of various unit operations for fluorination of uranium dioxide. The objective was to prepare ammonium uranium fluoride double salts from uranium dioxide and ammonium bifluoride, then decompose these salts to uranium tetrafluoride through heating to temperatures near 425 °C in either a fluidized bed or a stirred bed. Fluorination in the stirred bed was attempted without pretreatment of the reagents. For the fluidized bed experiments, reagents were ball-milled prior to being heated in the bed. Experiments were conducted in either argon or 4% hydrogen in argon.

The ball mill appeared to be an effective technique for fluorinating uranium dioxide with ammonium bifluoride. Samples changed color from brown to bright green, and no oxides could be detected in the x-ray diffraction pattern of the product.

It was found that stainless steel is a suitable material of construction for reaction vessels, whereas mild steel parts corroded quickly. Only a small degree of fluidization provided adequate mixing in fluidized beds, but a paddle mixing the stirred beds left an unmixed region around the bed perimeter.

Results from the stirred beds showed the initial fluorination reaction completed only when the reagents were heated to 110 °C for at least three hours under argon. Decomposition took place under argon with a temperature ramp up to 425 °C. The product UF_4 contained less than 1% oxide as an impurity, and the decomposition appeared to be complete.

Fluidized beds were run with both argon and 4% hydrogen in argon as carrier gases. Experiments with 4% hydrogen in argon produced uranium tetrafluoride, with ammonium uranium pentafluoride and uranium dioxide as impurties. Experiments in argon produced uranium tetrafluoride, with uranyl difluoride, ammonium diuranyl pentafluoride and triuranium octoxide as impurities. Minimum temperatures and times needed to decompose the double salt in the fluidized beds were 200 minutes at 115 °C, a 500-minute ramp to 425 °C, and 200 minutes at 425 °C. The intermediate double salt produced at 110 °C appeared to be triammonium uranium septafluoride.

Thesis Supervisor: Kenneth R. Czerwinski
Associate Professor, Department of Nuclear Engineering

Thesis Reader: John R. FitzPatrick
Technical Staff Member, Los Alamos National Laboratory

THIS PAGE INTENTIONALLY LEFT BLANK

Dedicated to Steve Yeamans, Bill Burnett, and David Pierce

In Los Alamos: Michael Martinez was absolutely indispensable, and without him I'm sure I never would have completed this project. Bobby Gonzalez, Gene Zimmerman, and Toby Romero got me the stuff to keep my equipment running, whether it had to be bought, made, borrowed, or "borrowed." Lorraine Vigil shoveled through the snowstorm of paperwork, and Louis Rivera kept me company, as was required by security regulations. Brad Shake made sure I had the tools and safety glasses I needed. Amy Cansteñeda did most of the preliminary work without being able to take much credit. The library staff humored my requests for obscure articles from long-defunct journals and found most of them among dusty storage room shelves.

In Cambridge: Karen Noyes, Gini Curran, and Jon Plaue know all the secret doors, cabinets, handshakes, signs, rooms, and forms it takes to navigate through MIT, as well as answering all of my stupid questions about where to find things. Mathieu Salanne translated all of my French and Belgian references, and for that I owe him a hamburger and French fries (which he informs me are actually Belgian). In addition to that, his work on the project I was supposed to be doing was nothing short of phenomenal, thus diverting enough attention from me to work on this one without harassment. Andy Gallant suggested enough changes to my experimental equipment such that it would actually be possible to construct, and then streamlined it through the machine shop ahead of all the undergraduate thesis projects.

The University of California, Berkeley Department of Nuclear Engineering will allow me to pursue my dream of cleaning up other people's radioactive garbage now that MIT has given up on it. Per Peterson talked me into being a nuclear engineer because it's important.

My advisor Ken Czerwinski, a.k.a. Flipper and a member of the LFHCfS, continues to be the grooviest cat ever to grace the sciences. He has given me the freedom to do this project for no better reason than I wanted to pursue it. As always, he sends his love. John FitzPatrick came up with this whole idea, and then let me take it with me.

I'd like to thank any deities and/or godlike entities who may have assisted me in this project, although no such help was solicited nor knowingly accepted.

Apologies: Susan KcKinney, I'm sorry I argued so much that you had to kick me out of high school chemistry. All molecular motion does cease at 0 °C and I was wrong to insist that it didn't. To the sociology department at Berkeley, sociology is not a "pseudoscience," nor is its research methodology "systematically and pathologically unscientific." I was wrong to say those things, among others, and I'm sorry I made your Sociology 3 professor cry. Louie Cernicek, sorry about your back yard, man. Next time I'll do a more thorough job of gluing the fins on the rocket. Mrs. Fox, I never should have flipped you off. That was very rude of me, even though you deserved it. Mrs. Dorin, it was petty of me to repeatedly suggest that it was both trivial and pointless to complete ream after ream of long-division practice sheets. I can't imagine where my life would be without long division... oh the long division I have done since then. You were right to give me even more reams of long-division practice sheets to teach me how to be a better human being. Oh, and I'm sorry I flipped you off, even though you deserved it. Principal Paluzcek, elementary school was not "a big fat waste of my time" and you and your teachers were not "glorified babysitters" and I'm sorry about attempting to tamper with your brakes. In addition, I apologize for making you spend so much time talking to me about my behavior. I can't help but think that if I had just been quiet, paid attention, walked on the sidewalk, followed the rules, and done as I was told I could have done something with my life... maybe even gone to college. Oh, and I'm sorry I flipped you off, even though you deserved it.

Contents

List of Figures

2.1 List of Tables

Chapter 1: Introduction

1.1 Motivation

Ammonium bifluoride (NH_4HF_2, also known as ammonium hydrogen fluoride) has been shown to fluorinate uranium dioxide (UO_2), and has been used successfully in the preparation of both tetravalent uranium fluoride salts and ammonium uranium fluoride double salts. Uranium dioxide can be converted to uranium tetrafluoride (known as "green salt" in the nuclear power industry) by a number of industrially accepted methods. The commonly deployed industrial processes use powerful fluorinating agents such as hydrogen fluoride at temperatures above 600 °C [1]. Since ammonium bifluoride is much less toxic than hydrogen fluoride, and the temperatures involved would be below 460 °C, it may prove a better industrial fluorinating agent. Equipment could be constructed from less exotic engineering materials; 300-series stainless steel is compatible with ammonium bifluoride whereas nickel or Monel is required to handle the more powerful fluorinating agents [2]. Uranium tetrafluoride can be reduced to uranium metal with calcium metal and iodine [3] and is also an intermediate in the production of uranium hexafluoride, used for isotopic enrichment of uranium by gaseous diffusion, through the Fluorox process reaction with air at 800 °C [4]:

$$2UF_4 + O_2 \rightarrow UO_2F_2 + UF_6$$

This work attempts to demonstrate, on a small scale, the feasibility of operating a fluidized bed process for the production of uranium tetrafluoride. Fluidized beds represent one of the most studied chemical engineering unit operations, but since the primary focus herein is on the applicability of this technology and not its optimization, very little effort has been devoted to fluidized bed performance relative to the ammonium uranium fluoride system thermochemistry. After finishing work with the stirred bed apparatus, it became apparent that a better method for keeping reagents well mixed while removing decomposition products would be necessary in order to develop an effective chemical process. The fluidized bed presents itself as the logical option since a carrier gas provides a means of agitation and heat transfer to reactants, while at the same time removing the more volatile decomposition products and excess reagents. A fluidized bed has a distinct advantage over a rotating drum, also commonly employed for processes involving solid-solid chemistry, in that it has no moving mechanical parts. Mechanical simplicity, from which reliability usually follows,

constitute the foundation of any practical chemical engineering process, and constitutes the primary motivation for use of a fluidized bed.

1.2 Experimental Overview

Uranium dioxide will be converted to uranium tetrafluoride by fluorination with ammonium bifluoride to form the intermediate double salt tetra-ammonium uranium octafluoride dehydrate, $(NH_4)_4UF_8 \cdot 2H_2O$. This double salt will then be thermally decomposed, yielding uranium tetrafluoride and ammonium fluoride.

The first objective of this project was to investigate the chemistry of the ammonium uranium fluoride system in a somewhat practical setting: the stirred bed reactor. Samples of reaction products were taken after both the initial fluorination and after decomposition of the double salt. At the intermediate stage, the primary impurity is oxygen remaining from incomplete fluorination of UO_2. Excess ammonium bifluoride reagent and ammonium fluoride may also be present. After the vessel was heated above 400 °C, decomposition should be complete, with partially decomposed ammonium uranium fluoride salts and uranium oxides as the primary impurities. Although a stirred bed demonstrated the chemistry, it fell short in enough practical areas to warrant development of a better unit operation.

The second, more practically applicable objective was to demonstrate this process in a fluidized bed reactor. The fluidized bed concept attempts to affect the same chemistry as the stirred bed, with analysis focused on the same points; however, it was necessary to first determine the proper operating conditions, in particular the gas flow rate, before an apparatus could be finalized. By first running a small sample in a glass chromatography column, visual observation confirmed proper bed fluidization. A full-scale glass column provided an exact analog for the final apparatus: a stainless steel column contained within a tube furnace to provide the full range of desired temperatures. The stainless steel column attempts to demonstrate effectiveness of the fluidized bed process for uranium fluorination, the materials compatibility of stainless steel with this process, and the suitability of pure argon or hydrogen in argon as a carrier gas.

Chapter 2: Background

2.1 Physical and Chemical Properties of Uranium Compounds

2.1.1 Oxides

Uranium dioxide is a brown or black solid with a cubic structure, melting at 2878 °C, and having a bulk density between 2.0 and 5.0 grams per cubic centimeter [5]. Finely divided uranium dioxide appears brown, whereas coarser-grained material appears black. Even small amounts of oxidation to higher oxides ($UO_{2+\delta}$) will also cause UO_2 to appear black.

Non-stoichiometric oxides of uranium, UO_{2+x}, where x is a continuous variable between 0 and 1, form spontaneously from the stoichiometric dioxide in the presence of oxygen (Figure 2.1). Tetrauranium nonoxide (U_4O_9, or $UO_{2.25}$), a black solid, constitutes a genuine phase in the phase diagram of uranium oxide. It forms slowly at 20 °C from uranium dioxide in the presence of oxygen. Uranium dioxide is most easily prepared from higher oxides by reduction with hydrogen at 300-600 °C. U_3O_8 is generally the most stable oxide of uranium in air. Even under conditions where U_3O_8 is not the stable phase, it is often formed since the reaction of UO_2 with oxygen is rapid compared to the reaction of U_3O_8 with oxygen.

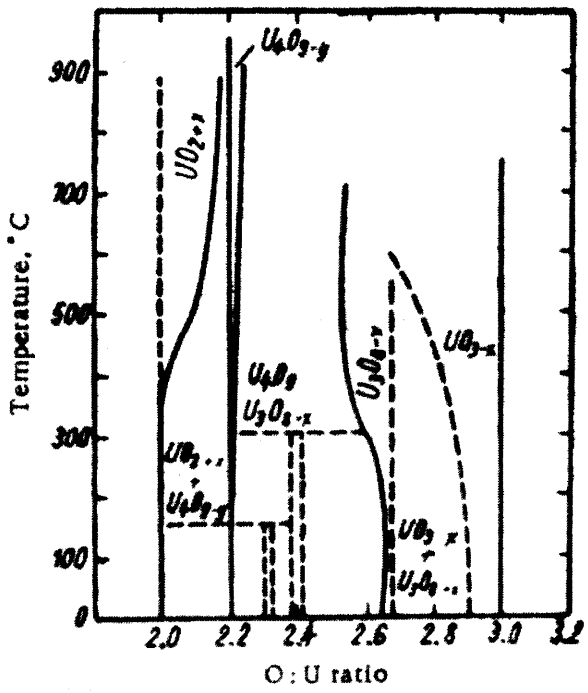

Figure 2.1 – *Phase Diagram of the Uranium Oxide System*: from Galkin NP, Sudarikov BN, et. al., Technology of Uranium, translated from Russian by USAEC, Springfield, Va : available from the U.S. Dept. of Commerce, Clearinghouse for Federal Scientific and Technical Information, 1966, p 18.

2.1.2 Fluorides and Ammonium Fluorides

Uranium tetrafluoride is a green solid with a slightly distorted square antiprismatic structure (eight-fold uranium-fluorine coordination, Figure 2.2). It melts at 960 °C and has a negligible vapor pressure at ambient temperature. Bulk density of the tetrafluoride is between 2.0 and 4.5 g/cc, depending on the method of preparation. UF_4 is stable in air up to at least 600 °C. The hydrated octafluoride double salt is a bright lime-green solid. Other ammonium uranium salts are light green.

Figure 2.2 – *Structure of Uranium Tetrafluoride*

Uranyl difluoride (UO_2F_2) is light yellow. It is stable in air up to 300 °C, after which it begins to decompose to U_3O_8. Above 110 °C, hydrated forms lose water to form anhydrous uranyl difluoride. It is highly soluble in water (65.6 weight % at 25 °C). Preparation is easiest from UO_3 and gaseous hydrogen fluoride at 300 °C, and can also be prepared with greater difficulty from aqueous solutions of UO_3 and hydrofluoric acid [6].

2.2 Chemical Behavior of the Ammonium-Uranium-Fluoride System

Uranium (IV) oxide and 10% excess ammonium bifluoride will react at 80-125 °C in an argon atmosphere to yield the dehydrated ammonium-uranium fluoride double salt $(NH_4)_4UF_8$ [7]. Ammonium bifluoride sublimes at 126 °C [8]. Although there is some debate as to the actual behavior of the chemical system, current knowledge indicates it behaves as described by Wani, Patwe, et. al. [9].

Fluorination:

1) $UO_2 + 4\ NH_4{\cdot}HF_2 \rightarrow (NH_4)_4UF_8{\cdot}2H_2O$
2) $(NH_4)_4UF_8{\cdot}2H_2O \rightarrow (NH_4)_4UF_8 + 2H_2O$

} 80-125 °C

Decomposition:

3) $(NH_4)_4UF_8 \rightarrow (NH_4)_3UF_7 + NH_4F$
4) $(NH_4)_3UF_7 \rightarrow (NH_4)_2UF_6 + NH_4F$
5) $(NH_4)_2UF_6 \rightarrow NH_4UF_5 + NH_4F$
6) $NH_4UF_5 \rightarrow UF_4 + NH_4F$

} 125-425 °C

Some older literature reports only NH_4UF_5 in the decomposing system, although the conditions described most likely lead to the formation of $(NH_4)_4UF_8$. Benz, Douglass, et al., [10] prepared samples of ammonium uranium fluoride compounds using a thermogravametric analyzer to control both temperature and atmosphere. Any sample that could be removed from the apparatus, remaining chemically and thermally stable, was considered a stationary arrest. Compounds inferred from their weight, but not actually removed and analyzed, were considered non-stationary arrests. Stationary arrests of $(NH_4)_2UF_6$, NH_4UF_5, and $NH_4F{\cdot}3UF_4$ as well as a non-stationary arrest of $(NH_4)_4UF_8$ were reported. Some experiments were done under argon, others under vacuum, but the decomposition was always reported to complete near 425 °C. The tetrafluoride is sufficiently stable to preclude decomposition of the tetrafluoride to the trifluoride [11].

Previous TGA studies of compounds in the ammonium uranium fluoride system suggest the existence of a large number of stable and metastable uranium tetrafluoride-ammonium fluoride compounds. Three polymorphic species were found for NH_4UF_5, while four were found for $(NH_4)_2UF_6$ [12]. The decomposition of ammonium uranium pentafluoride contains two discrete steps [13]. The heavier compounds, between $(NH_4)_4UF_8{\cdot}2H_2O$ and $(NH_4)_2UF_6$, are somewhat difficult to identify by TGA alone because one ammonium fluoride molecule has mass similar to two water molecules. Decomposition of the double salt can easily be confused with the loss of hydrate water from $(NH_4)_4UF_8{\cdot}2H_2O$. Modern literature sites crystallographic evidence that the system does contain the doubly hydrated octafluoride, and decomposition is sequential starting with the hydrate water and continuing to ammonium fluoride from the dehydrated compounds.

Powder x-ray diffraction patterns are known for most compound in the ammonium uranium fluoride system, with the most identifiable being the four phases of $(NH_4)_2UF_6$ (Figure 2.3). The distinct low 2θ peak may be used to identify this intermediate species, as no other ammonium uranium (IV) fluoride or uranium oxide has this peak. Ammonium uranyl fluoride compounds have their most intense peak between 11° and 13°.

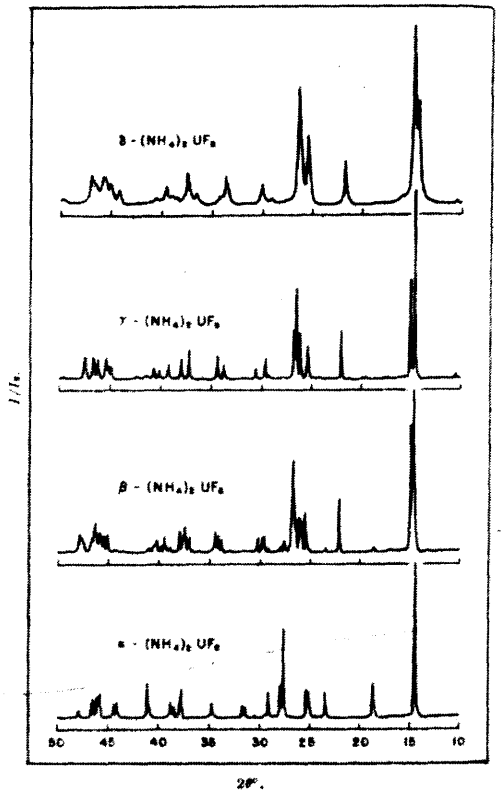

Figure 2.3 – *X-ray Diffraction Patterns of $(NH_4)_2UF_6$ Phases*: The peak just below 15° distinguishes these compounds from any other in the system of interest.
from Penneman RA, Kruse FH, et. al., Inorganic Chemistry, **3** #3 (1964), 309-315.

The use of ammonium bifluoride does raise the issue of solid-solid surface chemistry, but reaction kinetics are sufficiently fast if the reactants are finely ground and the bed is agitated during the reaction [14]. As a fluorinating agent, ammonium bifluoride is sufficient to fluorinate the tetravalent oxide, but will not, by itself, fluorinate tetravalent uranium to UF_6. As a reducing agent, no evidence is given for ammonium bifluoride reducing uranium oxides. Uranyl difluoride (UO_2F_2) will form when uranium dioxide reacts with ammonium bifluoride in the presence of oxygen in the range of 25-180 °C [15]. Uranyl difluoride also forms from the reaction of U_3O_8 and ammonium bifluoride in an inert atmosphere.

2.3 Common Methods for Preparation of Uranium Tetrafluoride

Uranium tetrafluoride can be prepared through the decomposition of ammonium uranium pentafluoride, NH_4UF_5, which is commonly prepared by precipitation from aqueous uranium solutions. Ammonium diuranate, $(NH_4)_2U_2O_7$, when reduced with zinc in hydrochloric acid, forms uranium tetrachloride dissolved in aqueous ammonium chloride. Upon treatment with aqueous hydrofluoric acid, ammonium uranium pentafluoride precipitates. This can then be filtered and dried [16]. In another aqueous process, ammonium uranium fluoride is precipitated directly from an aqueous uranium (IV) solution with aqueous ammonium bifluoride [17]. Mixtures of ammonium bifluoride and hydrazine fluoride have also been used to produce ammonium uranium pentafluoride [18]. The decomposition of ammonium uranium pentafluoride has been studied both on a laboratory scale, [19,20,21] and an industrial scale (see section 2.4). In the ammonium uranium (VI) fluoride system, double salts of ammonium fluoride and uranyl difluoride can be reduced to uranium tetrafluoride using a stream of Freon-12 (dichlorodifluoromethane) at 450-500 °C. [22]

2.4 Fluidized Bed Technology in Uranium Processing

A successful fluidized bed plant for the decomposition of ammonium uranium pentafluoride was built and operated in South Africa in the early 1960's. Feedstock was obtained from aqueous precipitation. Nitrogen was used to fluidize beds of approximately 500 kg of ammonium uranium pentafluoride per batch. Twenty six such batches were treated to produce UF_4 with less than 20 ppm nitrogen [23].

2.5 Fluidized Bed Behavior

Fluidized beds are common as unit operations in chemical processes involving solid-solid chemical reactions. A carrier gas is forced upward through a vertical bed of small solid particles, expanding and agitating the bed, giving it many properties of a liquid. In this state, powders can be made to flow through valves and piping, so fluidization is a common method of powder transport in the absence of a chemical reaction. When a reaction is desired, a fluidized bed provides the degree of homogenization required for high yields in a mechanically simple way compared to rotating blades or drums. Preheating the carrier gas

provides a simple method of temperature control within the bed, and due to the high degree of mixing, heat and mass gradients within the bed are virtually non-existent.

The degree and nature of bed fluidization depend largely on the properties of both the powder and carrier gas. The Archimedes number. Ar, Equation (2.1), is a representation of particle size.

$$Ar=d_p^{\,3}\cdot\frac{\rho\cdot\Delta\rho\cdot g}{\mu^2}=\left(d_p^{\,*}\right)^3 \tag{2.1}$$

A descriptive nondimensional fluid velocity is given by Equation (2.2).

$$U^*=U\cdot\left[\frac{\rho^2}{\Delta\rho\cdot g\cdot\mu}\right]^{\frac{1}{3}} \tag{2.2}$$

where

U	=	actual upward superficial fluid velocity, volumetric flow per total cross-sectional area
ρ	=	fluid density
$\Delta\rho$	=	difference between fluid density and particle theoretical density
μ	=	fluid viscosity
d_p	=	mean particle diameter
g	=	gravitational constant

Grace [24] gives a map describing bed operation within a wide parameter space of d* and U*. Particles are grouped based upon mean size and density. Uranium dioxide is generally in the form of Geldart Group B particles [25].

For spherical particles, the terminal fluid velocity, alternately interpreted as the velocity at which particles are entrained in the carrier gas stream and carried out of the bed, is approximately fifty times the minimum flow needed to fluidize the bed [26]. This gives a great deal of leeway in the operating parameters of a fluidized bed.

Different fluidization regimes (Figure 2.4) are characterized by an increasing bed void fraction as upward gas flow is increased. In the aggregative fluidization regime, individual particles remain largely in contact with one another, ideal for a bed in which a chemical reaction between two components is desired. A freeboard distance must be given above the top of the bed to allow for particles thrown up by normal spouting action to fall back into the bed without being carried out of the system. This can be estimated as the transport

disengagement height (TDH). For columns on the order of 0.01 m in diameter, the theoretical TDH is less than 0.1 m at all gas flows where aggregative fluidization occurs [27].

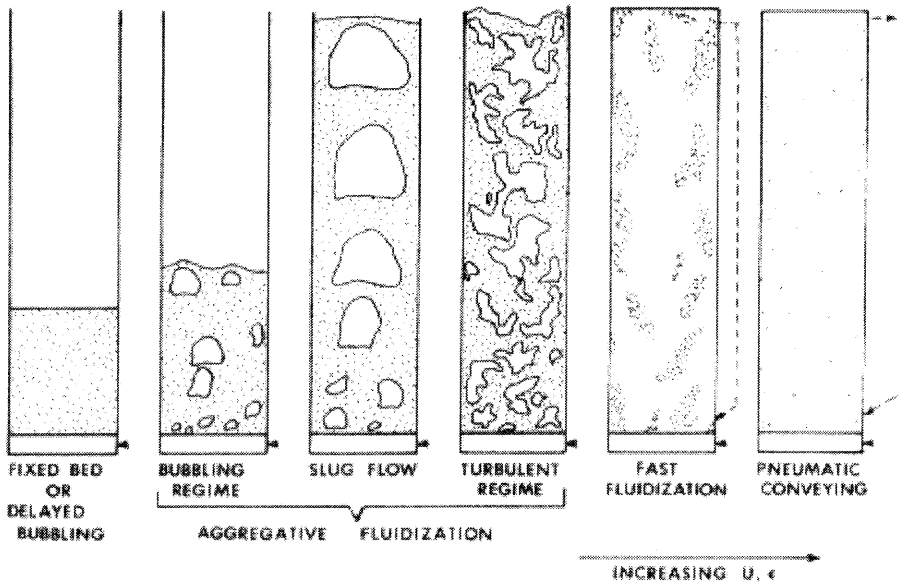

Figure 2.4 – *Flow Regimes for Upward Flow of Gas through a Particle Bed*: The aggregative flow regimes are ideal for bed in which a surface chemical reaction is desired.
(from Grace JR, Canadian Journal of Chemical Engineering, **64** (1986), 353-363.)

THIS PAGE INTENTIONALLY LEFT BLANK

Chapter 3: Experimental Equipment and Procedures

3.1 General Considerations

The decomposition of the ammonium-uranium fluoride system has been shown to take place at temperatures in the range of 425 °C. After all of the uranium oxide reacts to form the double salt, the temperature is ramped to ~425 °C to decompose the tetra-ammonium uranium octafluoride to produce an intermediate ammonium-uranium fluoride salt and ammonium fluoride. The bed is maintained at an elevated temperature to complete the decomposition of the salt to pure uranium tetrafluoride.

3.2 Experimental Descriptions

At ambient lab temperature (~20 °C), uranium dioxide and ammonium bifluoride were mixed both manually and mechanically. Heating of the reactants was carried out in both stirred and fluidized beds. Any experiment involving decomposition of ammonium fluoride double salts was done in a fume hood. Uranium oxide used in the stirred bed trial and the manually agitated ambient temperature trial was fairly coarse, thus the black color. For all other trials, the uranium dioxide used was Alfa-Aesar Lot #K22M14, 99.8% metal basis UO_2, finely divided (30 μm), brown in appearance. Ammonium bifluoride was supplied by Aldrich Chemical: 99.999%, Batch #14207AB. Both pure argon and 4% hydrogen in argon were supplied by BOC Gases.

3.2.1 Ambient Temperature Fluorination

3.2.1.1 Unagitated Reactants

At ambient temperatures (~20 °C), reactants can be mixed in Pyrex beakers because etching of glass by ammonium bifluoride is slow at these temperatures. Ammonium bifluoride rapidly etches glass at higher temperatures.

3.2.1.2 Manually Agitated Reactants

44.8 g of finely ground ammonium bifluoride was mixed with 52.4 g uranium dioxide. A small borosilicate glass beaker placed in a fume hood contained the reactants. Contents of the beaker were blended with a scoop once daily until the color was homogeneous throughout the mixture. Progress was monitored visually for a period of 17 days.

3.2.1.3 Mechanically Agitated Reactants

14.60 g uranium dioxide and 12.98 g ammonium bifluoride were placed in a ball mill (Spex Certiprep 8000M mixer/mill) for twenty minutes. The ball mill shakes the material contained in the vessel with several small stainless steel balls. The final product is finely divided but compacted, which was then ground by hand in an agate mortar to free the powder.

3.2.2 Stirred Bed

The reaction was attempted in a stainless steel stirred bed vessel (Figure 3.1) with a diameter of six inches surrounded by a tube furnace capable of producing temperatures up to 600 °C. The entire apparatus was contained within a ventilation hood to prevent personnel exposure to radioactive material and hazardous chemicals. A programmable electronic controller connected to a thermocouple maintained the furnace tube temperature within 10 °C of the setpoint. A separate thermocouple measured the temperature inside the reaction vessel. Finely ground ammonium bifluoride (88.2 g) was mixed with of uranium dioxide (100 g). An argon flow rate of 0.05 standard cubic feet per hour maintained an inert atmosphere within the reaction vessel. The temperature ramp began after loading material into the crucible, which was located near the bottom of the vessel. A Dayton 4Z435 gear motor, providing 26.2 in·lbs of torque at 7 rpm, turned a paddle with ¼" of clearance from the inside of the crucible. Mild steel shimstock (0.005") was added to the outside of the paddle blades in an attempt to eliminate the gap between the paddle blades and the crucible wall.

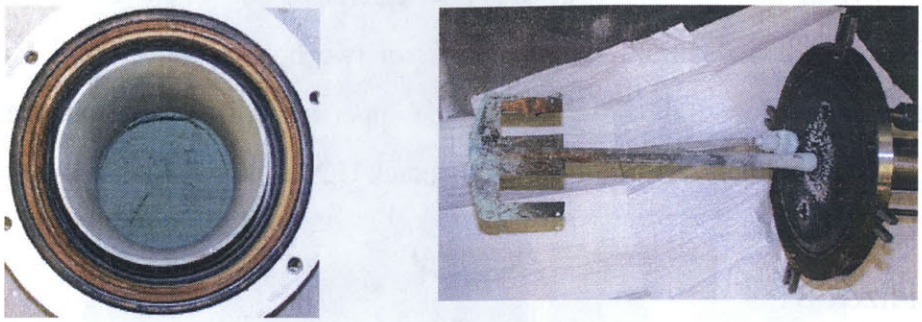

Figure 3.1 – *Stirred Bed Apparatus*: A crucible sat within the reactor vessel (left) and reactants were stirred by a paddle (right). The coating of rust visible in these pictures was the result of corrosion of mild steel shimstock that had been attached to the paddle to aid in complete mixing. Very little corrosion of stainless steel parts was seen.

Four different heating schedules were considered (Figure 3.2).

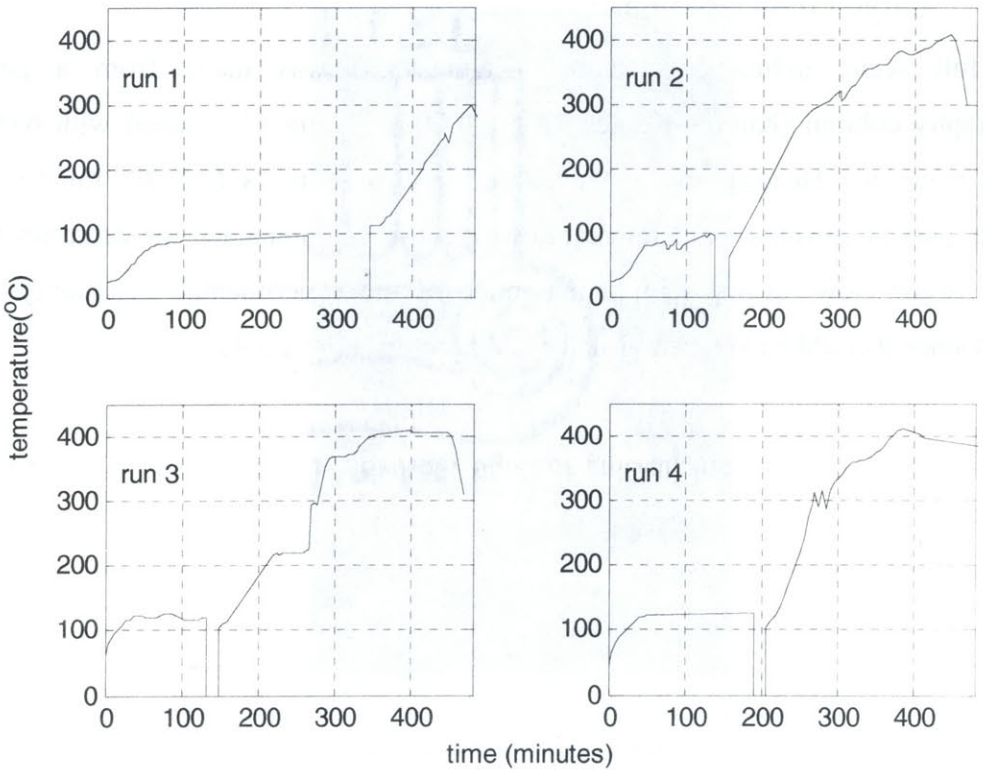

Figure 3.2 – *Heating Schedules for Mechanically Agitated Reactants:* These trials are characterized by the lower plateau temperature and duration, and the maximum temperature and duration.

Trials 1 and 2 held the sample at ~80 °C while trials 3 and 4 held the sample near 120 °C. Trial 3 held the sample above 400 °C for two hours whereas trial 4 allowed the temperature to drop below 400 °C for most of the upper temperature plateau. Samples from trials 1 and 2 were not analyzed due to distinctly black UO_2 visible in the final product.

3.2.3 Fluidized Beds

3.2.3.1 Small Glass Column

An 8.6 mm glass disposable chromatography column fitted with an argon flow line was loaded with 1.5 g UO_2 and 1.25 g NH_4HF_2. Argon was forced upward through the column frit at flows sufficient to fluidize the bed. The column was run in this manner at ambient temperature for ten days. Initial observations on the smaller column showed a significant variation between the calculated and actual bed properties.

3.2.3.2 Large Glass Column

A full scale, unheated apparatus (Figure 3.3) was made from a pesticide chromatography column (Kimble-Kontes 420600-0000, 22 mm ID) loaded with 6.08 g of ball-milled material. Heating was not available in this setup as NH_4HF_2 rapidly etches borosilicate glass at elevated temperatures; however, this setup enabled the determination of appropriate argon flow ranges, eliminating much of the experimental uncertainty in bed fluidization since it could be verified visually in this setup (Figure 3.4).

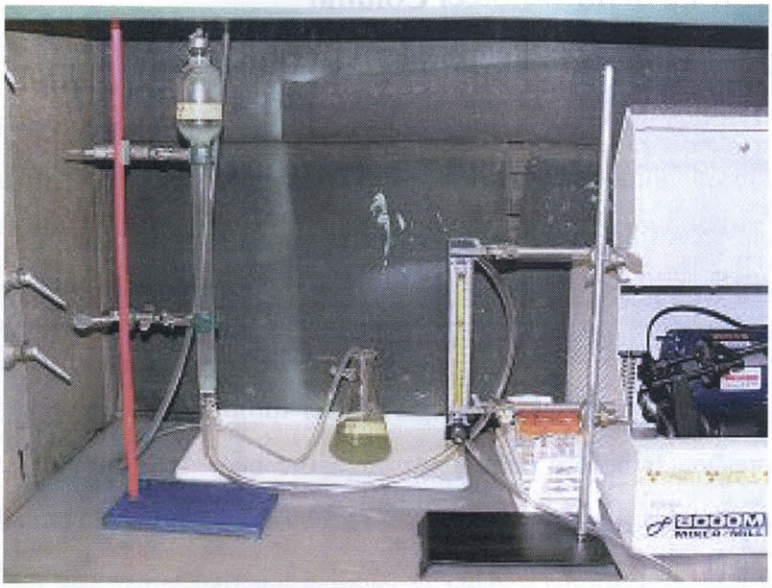

Figure 3.3 – *Full Scale Glass Column*: Argon flow is regulated and measured by the flowmeter at right, and flows upwards through the column at left. A water bubbler (at center) retains any uranium powder that may escape the system.

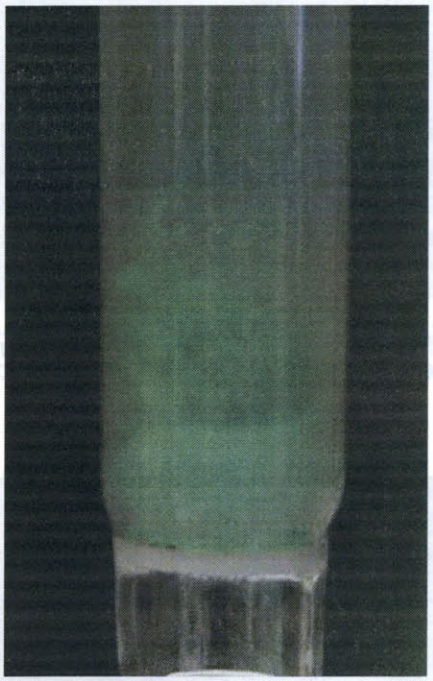

Figure 3.4 – *Detail of Full Scale Glass Column During Operation*: Fluidization is evident from the appearance of the bed.

3.2.3.3 Full-Scale Stainless Steel Column

3.2.3.3.1 Experimental Apparatus

The final setup constructed from stainless steel allowed for heating to achieve the full range of required temperatures. See Appendix A for detailed engineering drawings. The full-scale column consisted of a one-inch diameter 304 stainless steel pipe (Figure 3.5), mounted vertically and fitted with a 20 μm mesh disk (Figure 3.6) to support the bed. Fifteen inches of freeboard provided particle arresting, as did an expansion to two-inch diameter just upstream of the gas outlet. Carrier gas flowed through copper tubing wound around the outside of the main tube as a pre-heater before passing through the bed. The tube was supported in the center of a two-inch tube furnace (Barnstead/Thermolyne 21100), which kept the bed at a controlled temperature (Figure 3.7). Thermocouples inserted below the bed and at the top of the freeboard section measured temperature, recorded by a digital thermometer (VWR Double Thermometer with Computer Output #23226-656) fitted with Type K thermocouples.

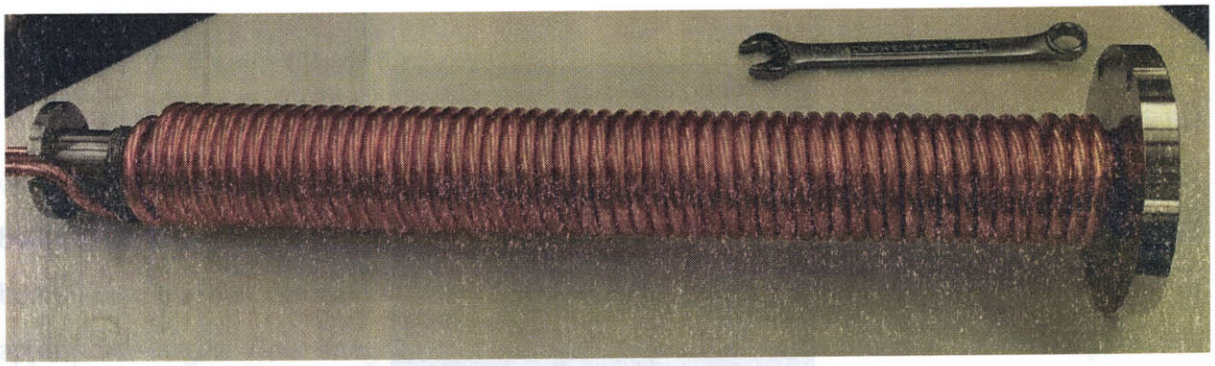

Figure 3.5 – *Main Column Piece*: Copper tube was wound around the column to act as a pre-heater for the inlet argon stream. The bed is located at the bottom of the column, which is on the far right side of this photo.

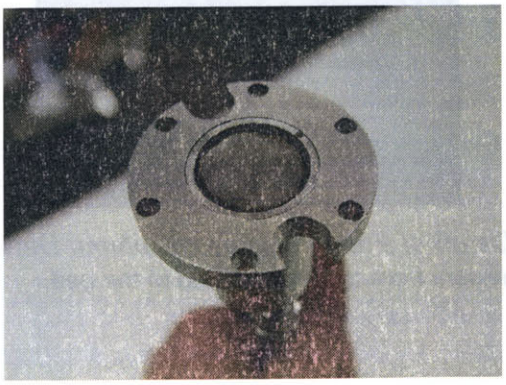

Figure 3.6 – *Frit Disk*

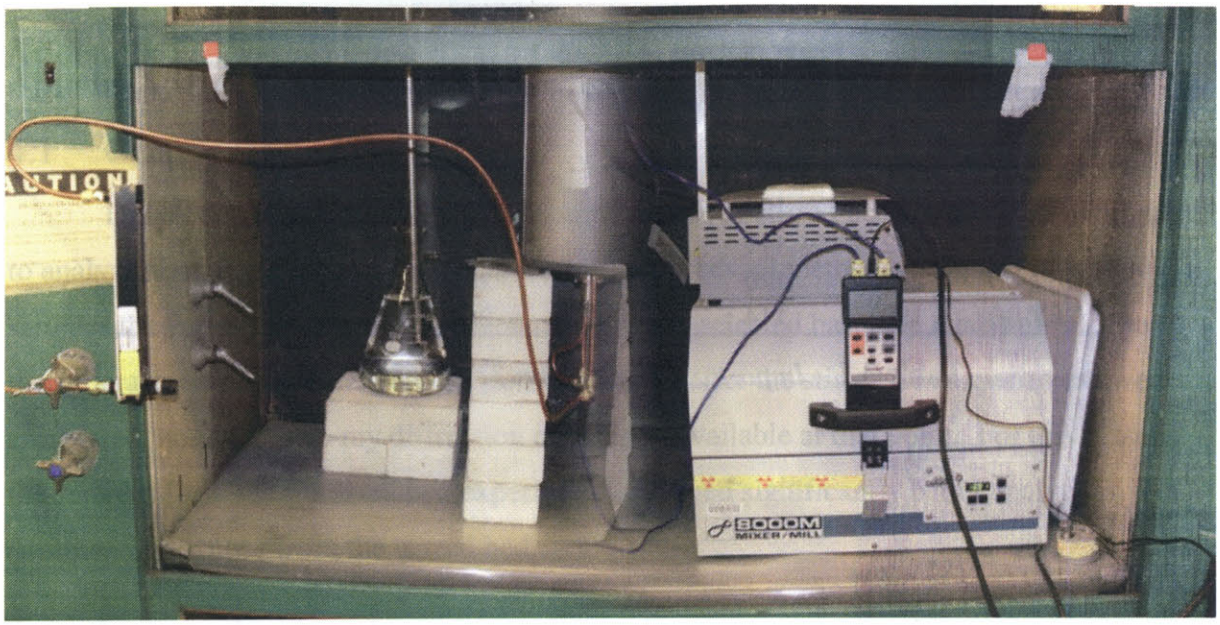

Figure 3.7 – *Full Scale Steel Column*: The entire setup was contained in a fume hood.

3.2.3.3.2 Temperature Monitoring and Control

Rigid Type K thermocouples were mounted at both ends of the column. The primary thermocouple sat about 1/8" below the bed, vertically in the gas stream. A secondary thermocouple measured temperature near the column outlet, just above the top column flange. Temperature was controlled by the built-in controller (Eurotherm 2116) on the furnace. Furnace tube temperature could be set, as well as ramp rates and dwell times. Since the temperature difference between the furnace tube and the bed varied slightly between trials, furnace setpoints were adjusted accordingly to maintain proper bed temperature.

3.2.3.3.3 Temperature Cycles

Heating cycles were designed to heat the bed to a lower plateau temperature within five degrees of 115 °C. Upper plateaus were designed to hold the bed within five degrees of 425 °C. Hold times are given for the actual measured values, not set dwell times, and are reported based on the time for which the measured temperature was within two degrees of the given bed temperature value. The outlet temperature responded much more slowly to changes in furnace tube temperature, thus the actual outlet temperature hold times were less than those for the bed temperature. Table 3.1 contains important parameters for heating cycles used. Figure 3.8 plots a typical heating cycle.

	lower plateau			upper plateau		
sample	time (min)	bed temp	outlet temp	time (min)	bed temp	outlet temp
CBY-01	112	81	68	132	427	257
CBY-02	64	101	n/a	156	439	183
CBY-03	186	108	80	116	437	185
CBY-04	172	111	73	n/a	n/a	n/a
CBY-05	245	120	75	238	428	179
CBY-06	190	114	91	262	426	215

Table 3.1 – *Important Values from Temperature Cycles*

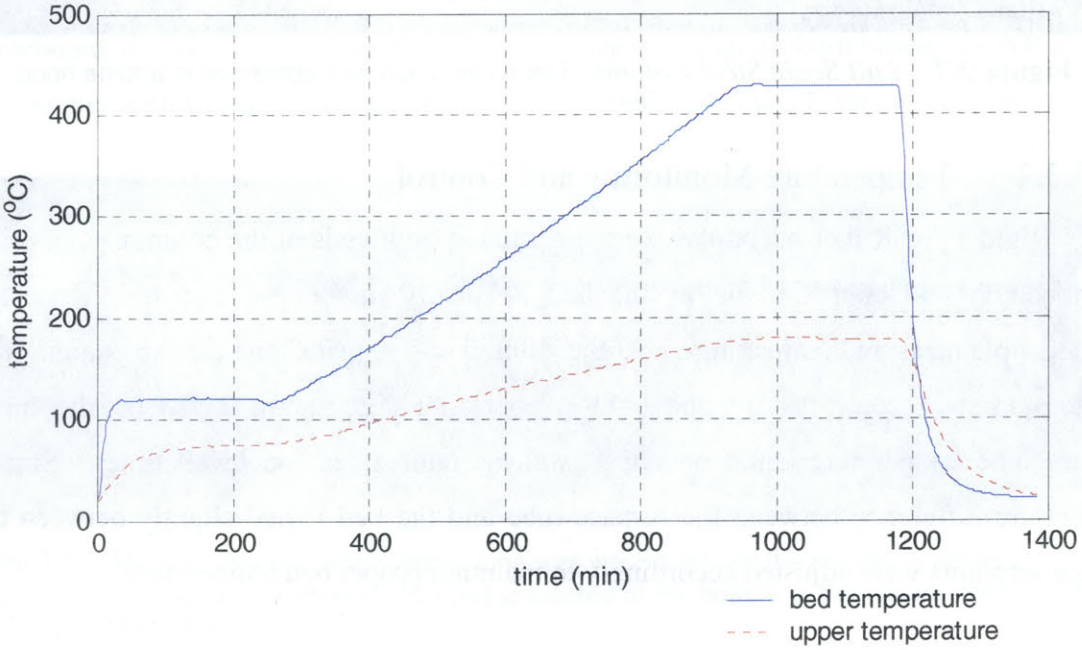

Figure 3.8 – *Measured Temperatures versus Time for Sample CBY-05*

3.2.3.3.4 Feedstock

Most fluidized bed samples (CBY-02 through CBY-06) were prepared using a ball-milled mixture of ammonium bifluoride and uranium dioxide with 2.37% excess ammonium bifluoride by weight. Sample CBY-01 was prepared from a similar feedstock that had not been ball-milled.

Chapter 4: Analytical Methods

4.1 General Comments

Different analytical methods were used to analyze stirred bed samples than were used to analyze fluidized bed samples. This chapter describes all methods used, and to which samples they apply. In general, the method used was selected based on availability. The thermogravametric analyzer was not purchased until after the stirred bed experiments were completed, nor was the x-ray diffraction equipment available at that point. For this reason, the samples from the fluidized bed experiments received significantly better analytical treatment than those from the stirred bed.

4.2 Uranium Mass Fraction

For samples prepared in the stirred bed reactor, uranium mass fractions were determined by liquid scintillation counting.

For those prepared in fluidized beds, a small sample, in the range of 10mg, was removed and dissolved in 10mL concentrated nitric acid. The dissolved sample was diluted with de-ionized water to 25 mL in a volumetric flask. This solution was transferred to a scintillation vial from which 1mL of solution was pipetted to a separate vial with 7mL of dionized water. This brought the uranium and acid concentration into a proper range for inductively-coupled plasma atomic emission spectroscopy (ICP-AES), usually 0.01 to 0.05 grams uranium per liter. The ICP-AES instrument used was a SpectroFlame PMC FMD-07 (SN 4605/92). Calibration curves were obtained for each session from standard samples prepared by dilution of a PlasmaCAL 1000 μg/mL uranium standard (Lot SC223591).

4.3 Soluble Uranyl Fluoride Content

To exploit the solubility difference between uranium (IV) and uranium (VI) compounds, water dissolution was performed to determine the fraction of uranium in water soluble species. 25 mg samples were dissolved in dionized water. After nine hours, these samples were diluted to 25 mL and the uranium concentration measured using ICP-AES.

4.4 Oxygen Content

Material prepared in the stirred bed were analyzed for oxygen content by heating samples in a graphite crucible to 1000 °C under an inert atmosphere. The CO concentration was then measured, and the oxygen content of the sample interpolated using a calibration curve.

4.5 Nitrogen Content

Samples prepared in the stirred bed were analyzed for total nitrogen content by ion chromatography. Free NH_3 and soluble NH_4^+ was determined by water dissolution, followed by ion chromatography.

4.6 Thermogravametric Analysis

Thermogravametric analysis was performed on a Perkin Elmer, Pyris 1 TGA using sample sizes between 5 and 40 mg. There was no offgas analysis. Details of heating cycles are provided with each data set in the lower part of all TGA data figures. Argon was used as both a blanket gas and pneumatic gas. There was no oxygen removal system on the gas inlet.

4.7 X-Ray Diffraction

X-ray diffraction patterns were obtained with a Rigaku RU200 x-ray tube with a rotating copper anode. The copper $K_{\alpha 1}$ line was used for the analysis in a 185 mm diffractometer. Samples were run using the maximum power available from the tube: 18 kW, operating at 60 kV and 300 mA. Sample scans covered a 2-theta range from ten to one hundred degrees, and patterns were analyzed using JADE (version 5.0) software. This software removed amorphous background peaks and $K_{\alpha 2}$ lines from the raw pattern. Output is a list of possible matches to known compounds based on the observed pattern. This software contained powder diffraction files for most uranium compounds, but these files were listed as "questionable." Data analysis takes on a much more heuristic character with the apparent lack of reliable data, as patterns from unknown samples could be compared to those obtained with standard uranium compound samples. Similar peak locations and sizes can be compared, but no quantitative analysis can be performed with this method.

Corundum (Al_2O_3) was added to samples in order to calibrate the 2θ axis. Corundum lines are present in all XRD patterns. The stronger lines contained in the JADE powder diffraction file are shown in Table 4.1.

2θ	I/I_o
25.578	0.45
35.152	1.00
37.776	0.21
43.355	0.66
52.549	0.34
57.496	0.89
61.298	0.14
66.519	0.23
68.212	0.27
76.869	0.29
77.224	0.12

Table 4.1 – *Strong X-ray Diffraction Peaks of Corundum*

THIS PAGE INTENTIONALLY LEFT BLANK

Chapter 5: Results

5.1 Fluorination of Uranium Dioxide

5.1.1 Unagitated Reactants

Experiments at ambient temperature (~20 °C) demonstrated that fluorination of UO_2 to $(NH_4)_4UF_8 \cdot 2H_2O$ progresses slowly: visible amounts of unreacted UO_2 and $NH_4 \cdot HF_2$ remained after 17 days (Figure 5.1). When heated to near 125 °C, this reaction proceeds quickly.

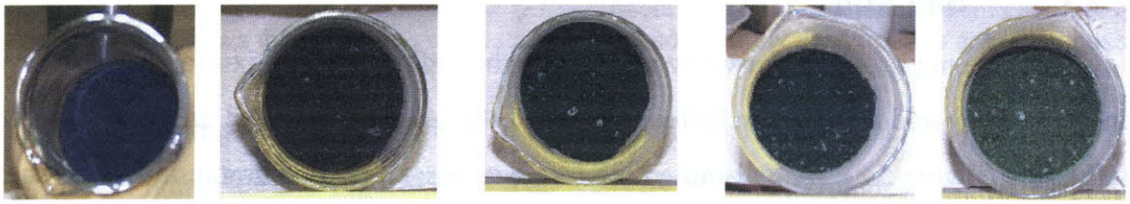

0 days **2 days** **10 days** **14 days** **17 days**

Figure 5.1 – *Ambient Temperature Fluorination*: The reaction between ammonium bifluoride and uranium dioxide progressed slowly at room temperature, evident by the slow change from black uranium dioxide to the green ammonium fluoride double salt.

5.1.2 Mechanically Mixed Reactants

5.1.2.1 Stirred Bed

Because no samples from the stirred bed were taken before the heating cycle began, any conclusions about the effectiveness of fluorination must be made based upon samples from intermediate decomposition stages. Oxides in the intermediate may be left over from incomplete fluorination or come from oxygen in the cover gas. Based on the visible presence of uranium oxides in stirred bed trials 1 and 2 (Figure 5.2), and the lack of visible oxides in trials three and four, it appears that three hours at 80 °C is not sufficient to allow the fluorination reaction to go to completion if the reactants are not finely ground.

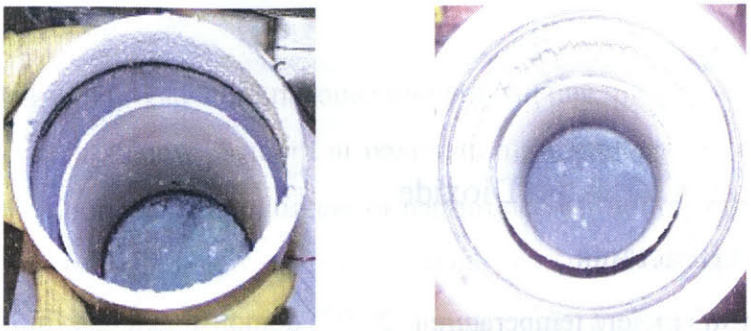

Trial #1 Trial #2

Figure 5.2 – *Product After Incomplete Fluorination in Stirred Bed:* Black UO_2 powder is visible in green UF_4. The fluorination reaction is slow at 80°C.

5.1.2.1 Ball Mill

After being ground for twenty minutes in the ball mill, the mixture of finely divided uranium dioxide and ammonium bifluoride turned the color of hydrated ammonium uranium octafluoride (Figure 5.3). A ball-milled mixture with larger-grained uranium dioxide showed no color change initially (Figure 5.4); however, after being left for 24 hours, the color of the mixture was similar to that of the product from the experiment with finer uranium dioxide.

Figure 5.3 – *Ambient Temperature Fluorination, Fine UO_2*: When the brown reagents (left) were ground in a ball mill for twenty minutes, a pronounced color change to bright green (center) occurred. After the powder was fluidized in argon for two days, the color was slightly lighter (right).

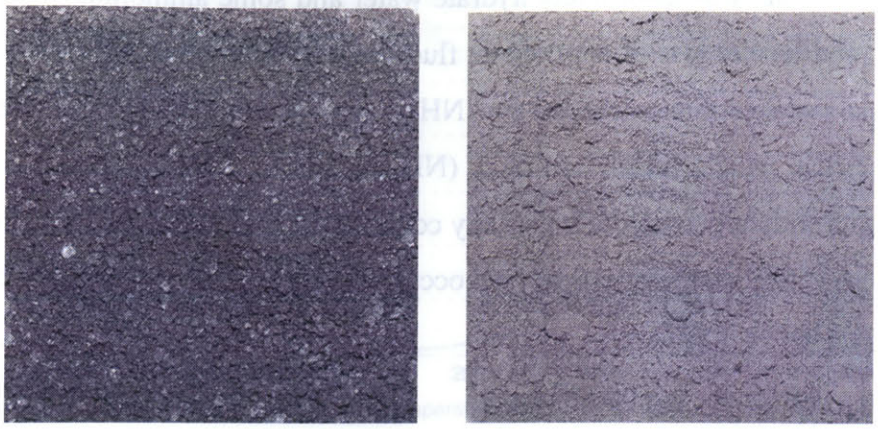

Figure 5.4 – *Ambient Temperature Fluorination, Coarse UO_2*: When black UO_2 and NH_4HF_2 (left) were ground in a ball mill for twenty minutes, no color change occurred initially (right). After twenty four hours, the color was similar to that of the product from finer-grained uranium dioxide. The larger particle size slows the fluorinations reaction, but not so severely as to impede actual processing.

Samples prepared using the ball mill from both coarse and fine UO_2 were analyzed using TGA (Figure 5.5 and Figure 5.6). The analysis of Benz, Douglass, et. al., used TGA run times near 1000 hours, but since this amount of time was not available, shorter runs were used. Different heating cycles were used in an attempt to economize time expenditure, and since later analysis revealed both ball-milled samples to be the same material, TGA data was interpreted assuming analysis of one sample could be applied to the other. The first heating cycle used appeared to be too fast to allow for the decomposition steps to complete in a discrete and identifiable manner, so a slower heating cycle was used. Theoretical weight fraction values for TGA of $(NH_4)_4UF_8{\cdot}2H_2O$ are shown in Table 5.1.

species	composition					molecular weight	fraction of initial wt.
	U	F	NH_4	H_2O	O		
$(NH_4)_4UF_8{\cdot}2H_2O$	1	8	4	2	0	498.2	≡1.000
$(NH_4)_4UF_8$	1	8	4	0	0	462.1	0.928
$(NH_4)_3UF_7$	1	7	3	0	0	425.1	0.853
$(NH_4)_2UF_6$	1	6	2	0	0	388.1	0.779
NH_4UF_5	1	5	1	0	0	351.0	0.705
UF_4	1	4	0	0	0	314.0	0.630
UO_2	1	0	0	0	2	270.0	0.542

Table 5.1 – *Theoretical Weight Loss Values for Compounds in the Ammonium Uranium Fluoride Double Salt System*: These values correspond to the blue dashed lines drawn on subsequent TGA plots.

A loss of what was most likely hydrate water and some ammonium fluoride occurred below 80 °C, and further loss of ammonium fluoride continued up to 110 °C. At 110 °C, the product weight matched that calculated for $(NH_4)_3UF_7$. Another distinct loss step began near 150 °C with a final weight matching that of $(NH_4)_2UF_6$. All weight loss steps above 200 °C did not lead to a weight corresponding to any compound observed in the ammonium uranium fluoride system. The sharpest weight loss occurred at 278 °C, with one additional distinct step starting just above 300°C.

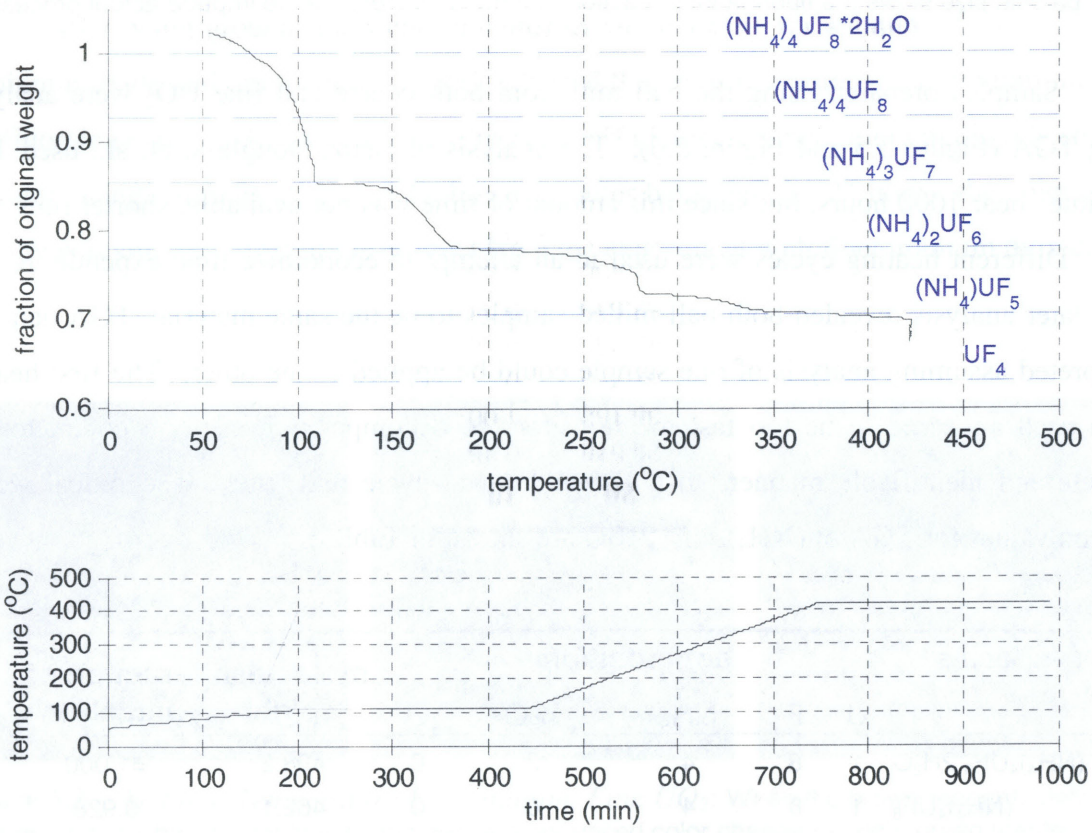

Figure 5.5 – *TGA Curve of Ball-Milled Sample*: (upper) Dashed lines show theoretical plateau values for various intermediate compounds in the ammonium uranium fluoride system. The curve starts above a mass fraction of one to account for removal of excess ammonium bifluoride. The lower plot shows the heating cycle used.

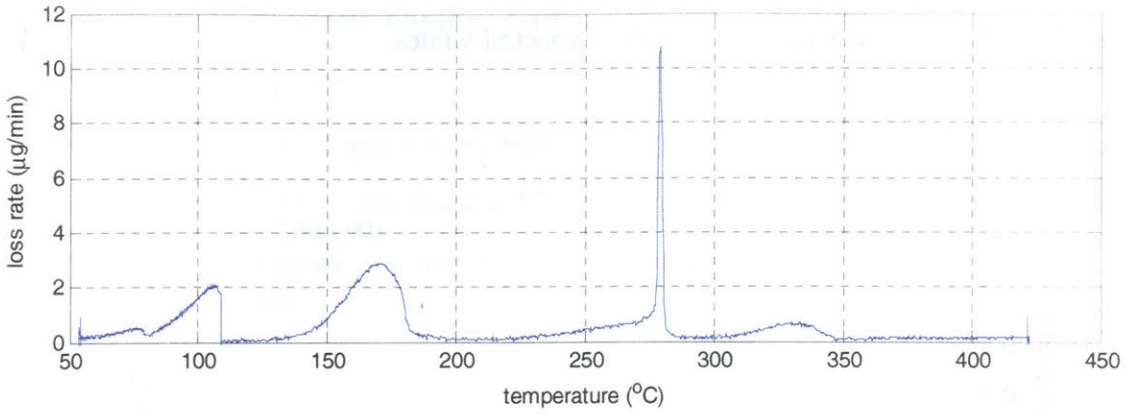

Figure 5.6 – *TGA Weight Loss Rate Curves of Ball-Milled Samples*: Rate of weight loss is plotted versus temperature. Five distinct weight loss steps are observed.

Since no powder diffraction file existed for the hydrated double salt, these samples could only be analyzed for the presence of uranium oxides. It was assumed interference from the pattern of $(NH_4)_4UF_8 \cdot 2H_2O$ would not be strong enough to preclude the observation of uranium oxides, and that a pattern in which no uranium oxides were detected was sufficient evidence for complete fluorination. No uranium oxides could be identified in the XRD spectra of the ball-milled products.

5.1.2.3 Small Fluidized Bed

Samples produced in the small fluidized bed were light green in color and showed no visible signs of dark UO_2. XRD analysis did not identify the compound formed, but identified excess NH_4HF_2, and did not identify the presence of UO_2 (Table 5.2). No powder diffraction file existed for the hydrated double salt, $(NH_4)_4UF_8 \cdot 2H_2O$, therefore it is possible for the compound to be present without being identified.

pattern match	figure of merit	comment
Corundum, Al_2O_3	6.3	standard used for 2θ calibration
NH_4HF_2	25.9	excess reagent
$Al(OH)_3$	32.4	spurious match
$Al_6O_3N_4$	43.6	spurious match
Aluminum Oxide, Al_2O_3	39.8	likely from corundum standard

Table 5.2 – *Search Match List for Small Column Samples*: Only excess ammonium bifluoride and corundum were identified in the small column sample. No uranium oxides were matched, demonstrating the completeness of the fluorination reaction after one week without any mechanical grinding of the reagents.

TGA curves from small column samples (Figure 5.7) showed at least three distinct weight loss steps, but weight loss exceeded expected values.

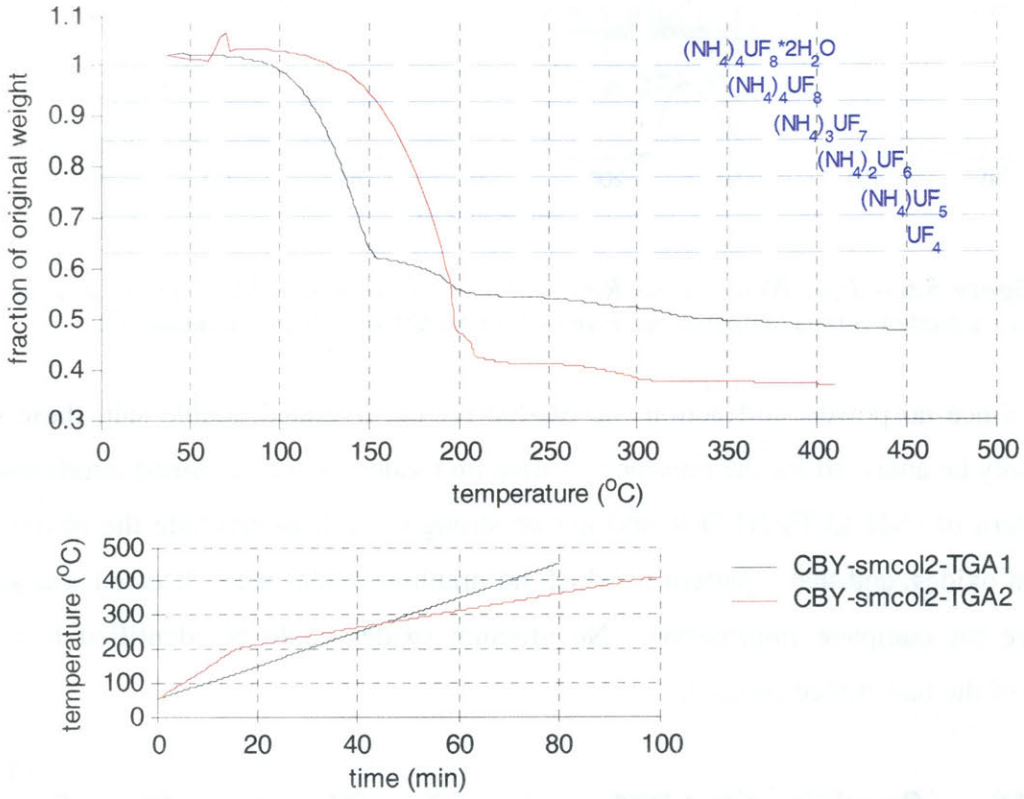

Figure 5.7 – *TGA Curves of Small Column Samples*: At least three distinct weight loss steps are evident. The second trial, CBY-smcol2-2, was an attempt to gain greater resolution in the higher temperature region by slowing the ramp rate. Weight loss exceeds expected values.

5.2 Decomposition of the Double Salt

5.2.1 Stirred Bed Reactor

Samples from trials 3 and 4 were taken after the lower heating plateau and from the final product. These samples were dried at 120 °C to remove atmospheric water and analyzed for oxygen and nitrogen impurities, and for overall uranium content (Tables 5.3 and 5.4).

sample	uranium (g/g)	oxygen (ppm)*
intermediate run #3	0.5155	270
intermediate run #4	0.5187	1700
pure $(NH_4)_4UF_8$	0.5149	0
99% $(NH_4)_4UF_8$ with UO_2 as the impurity	0.5171	1000

* assuming UO_2 is the only impurity present at this stage

Table 5.3 – *Impurity Analysis on Intermediate Products from Stirred Bed Experiments*

sample	uranium (g/g)	oxygen (ppm)	Nitrogen (μg/g)	
			Total	NH_3/NH_4^+
product run #3	0.7480	640	3900	530
product run #4	0.7207	910	15100	3700
pure UF_4	0.7580	0		
Paducah UF_4		~1000		

Table 5.4 – *Impurity Analysis on Final Products from Stirred Bed Experiments*

5.2.2 Fluidized Bed

5.2.2.1 Intermediate Product

Samples removed from the column after a dwell time of 172 minute at 110 °C were analyzed to determine the chemical speciation at this temperature and to detect signs of uranium oxides. UO_2 produces a simple x-ray diffraction pattern (Figure 5.8), with the most intense peak at 28.2°, and is easily identified by JADE (Table 5.5). Scans were run over a 2θ range from 10° to 100°.

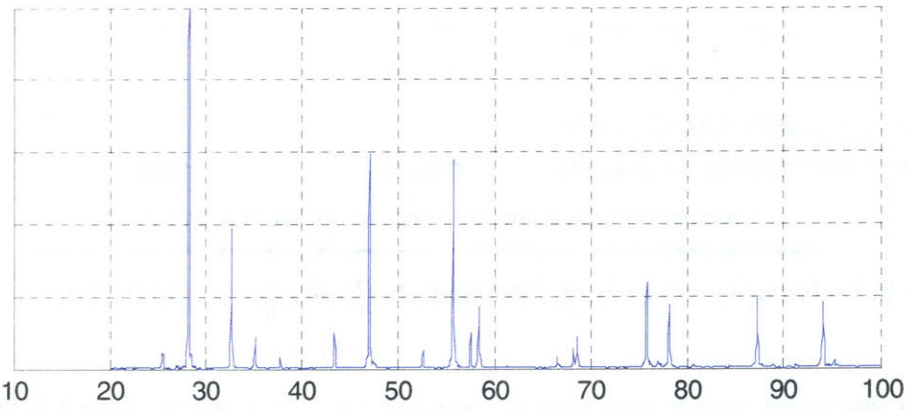

Figure 5.8 – *X-Ray Diffraction Pattern of UO_2 with Corundum Standard, Intensity versus 2θ.* This pattern was obtained from UO_2 used as a starting material. Although this scan begins at 2θ=20°, no significant peaks exist below 20° in the pattern of UO_2.

pattern match	figure of merit	comment
UO_2	1.7	likely species
Corundum, Al_2O_3	6.0	standard used for 2θ calibration

Table 5.5 – *Search Match List for UO_2 Sample*: UO_2 and the corundum standard were the only likely species identified by x-ray diffraction.

TGA curves of the intermediate product (Figure 5.9) yield no useful information on the composition of the intermediate. Since no oxygen trap was installed in the inlet line to the TGA, oxidation of the sample may have occurred, and would explain the constant weight loss slope apparently superimposed over the discrete steps of the double salt decomposition.

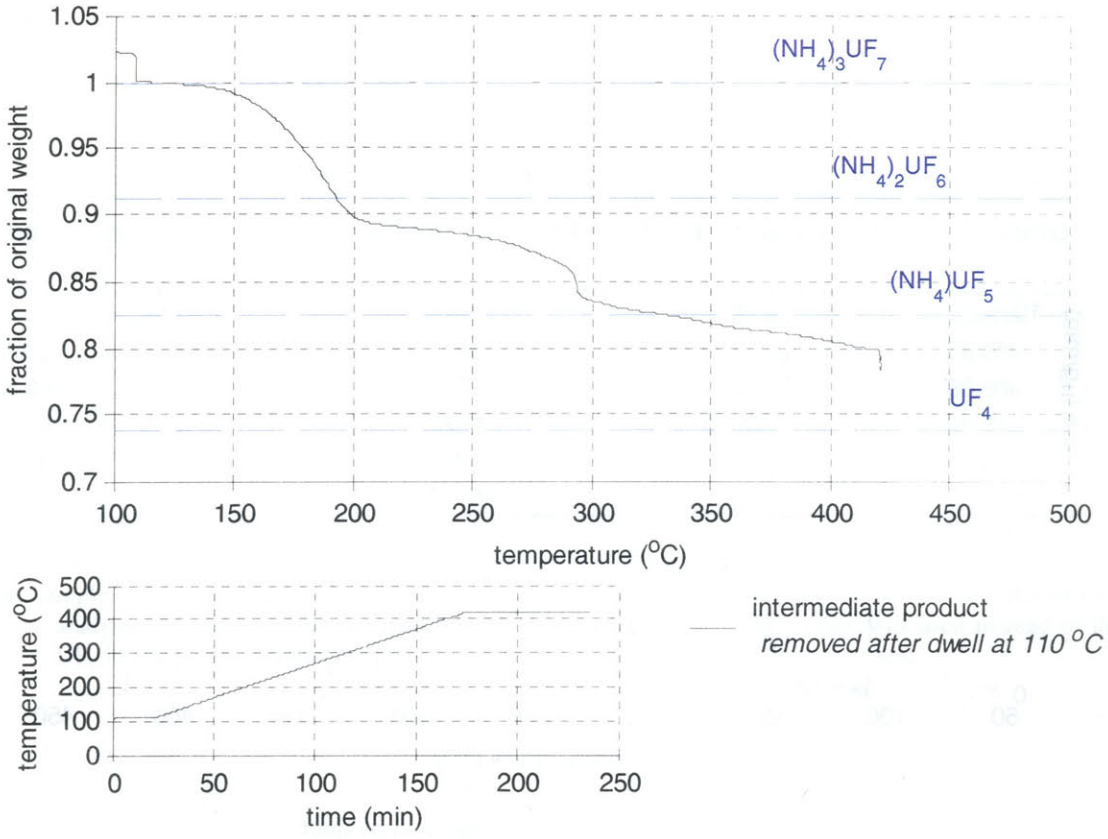

Figure 5.9 – *TGA Curve of Intermediate Product Sample, Removed at 110 °C*: This sample was removed from the column after the dwell period at 110 °C. Product is expected to be an ammonium uranium fluoride double salt close in stoichiometry to $(NH_4)_3UF_7$.

By comparing the rate of weight loss from an intermediate sample to that of a ball-milled sample, it is possible to determine if the intermediate decomposes through the same steps as the starting material once the starting material has been brought to the temperature at which the intermediate was made. Figure 5.10 shows such a plot; however, the ramp rates for the two samples were different. This means the plots cannot easily be directly compared. It can be seen that the plots do have similar features, with those for the intermediate being more spread out along the temperature axis. This follows from the intermediate analysis being done at a faster ramp rate than for the starting material.

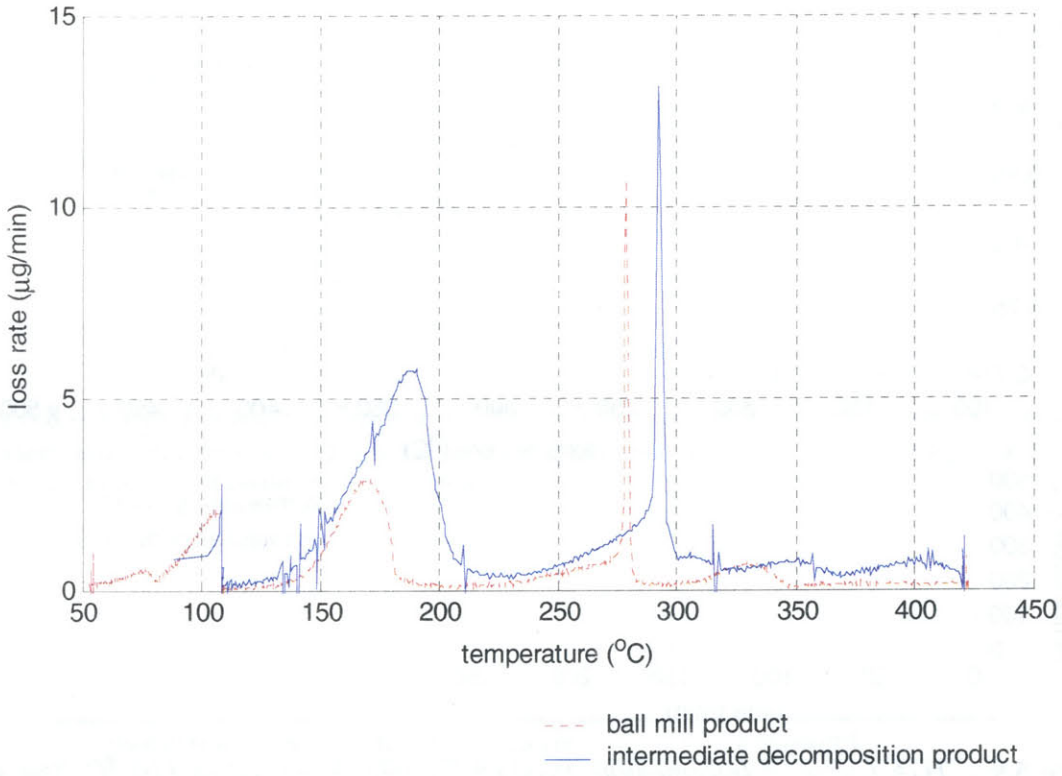

Figure 5.10 – *TGA Weight Loss Rate Curve of Intermediate Product*: Rate of weight loss is plotted versus temperature. Features appear similar to those in the plot for the ball-milled samples, but since ramp rates and sample sizes were different (2 °C per minute for the intermediate versus one °C per minute for the bal milled sample), the two plots cannot be directly compared.

5.2.2.2 Final Product: UF_4

After the full heating cycle, samples were typically light green in color with a visible coating of darker material on the outside of particles and clumps of particles. Interior areas of larger particle clumps contained no brown or black uranium oxides, indicating the oxygen source was most likely external to the bed. For samples prepared in argon, the darker color was black. The sample prepared in 4% hydrogen had a brown coating. Yields were above 97.8% once carrier gas flow (Appendix E) was lowered to the channelized fluidization regime.

Table 5.6 – *Masses and Yields of Fluidized Bed Samples*

sample	initial mass	theoretical UF_4 yield	actual final mass	gross yield
	g	g	g	
CBY-01	2.8042	1.7248	1.2749	73.9%
CBY-02*	2.7958	1.7196	1.3508	78.6%
CBY-03	2.857	1.7573	1.5275	86.9%
CBY-04†	2.8018	2.3333	2.3036	98.7%
CBY-05	2.8218	1.7356	1.6982	97.8%
CBY-06	2.814	1.7308	1.72282	99.5%

* Since the high argon flow rate carried a large amount of the sample onto the top flange of the column, the number given here is the sum of both samples CBY-02a (top flange) and CBY-02b (bed).

† This sample was an attempt to decompose the sample to its intermediate product at 110 °C. Based on TGA analysis, the intermediate product appears to be $(NH_4)_3UF_7$, so this value was used instead of that for UF_4 in calculating theoretical yield.

Final product samples from beds fluidized by both argon and 4% hydrogen in argon were analyzed with a simple TGA heating ramp. Pure UF_4 should show only a slight weight loss at elevated temperatures due to sublimation of pure UF_4 (Figure 5.11).

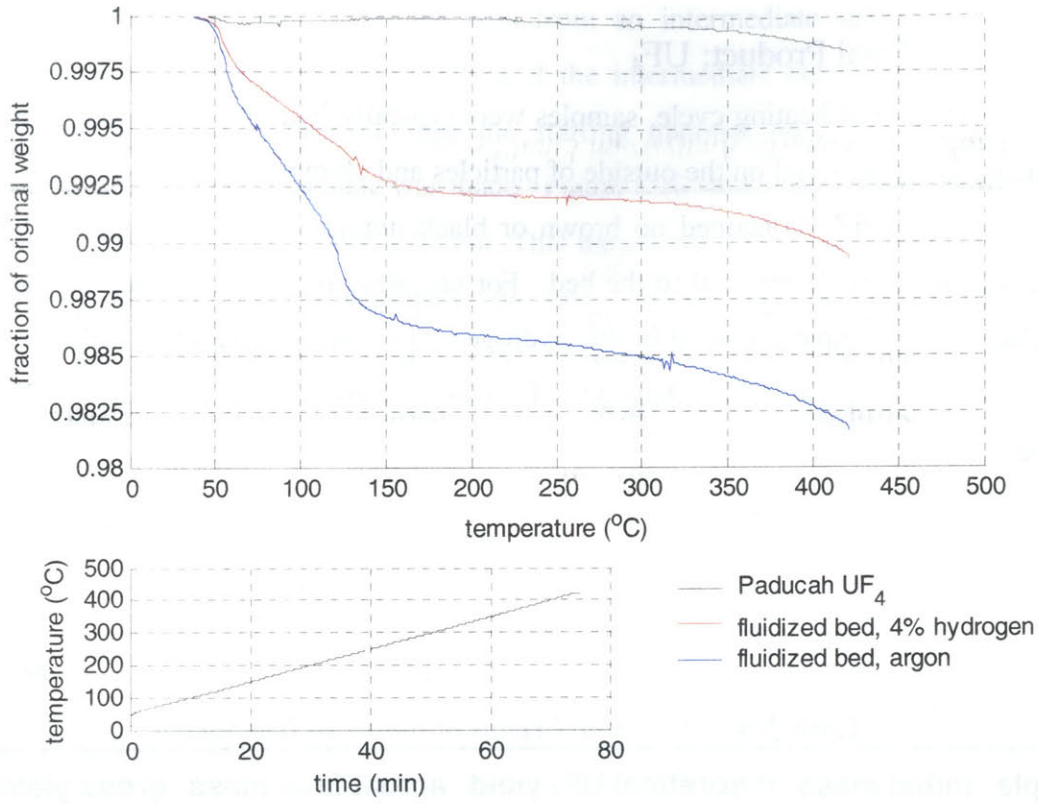

Figure 5.11 – *TGA Curves of Final Product Samples*: Samples prepared in the fluidized bed were compared against a UF_4 standard. The sample prepared in 4% hydrogen showed a 0.7% weight loss over the standard while a sample prepared in argon showed a 1.6% loss.

X-ray diffraction analysis looked for the primary pattern of UF_4, trace patterns of UO_2 and U_3O_8, ammonium uranyl fluoride compounds, and ammonium uranium fluoride compounds. The measured x-ray diffraction pattern of UF_4 is given in Figure 5.12, and search match results in Table 5.7. UF_4 is clearly identified.

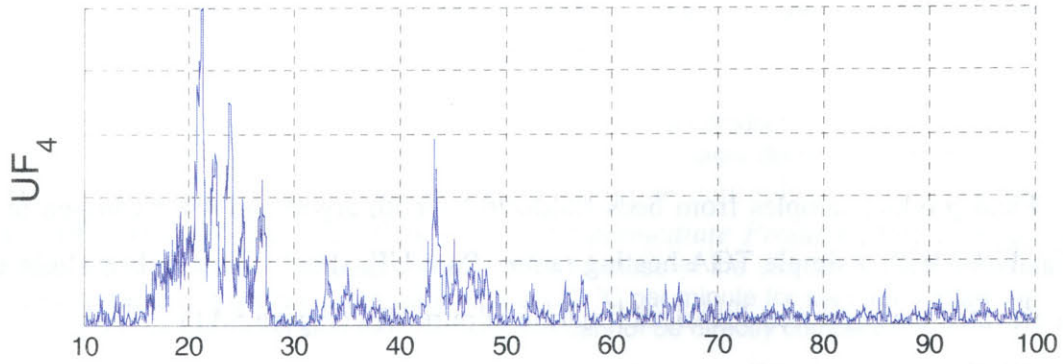

Figure 5.12 – *X-ray Diffraction Pattern of UF_4 with Corundum Standard, Intensity versus 2θ.* This pattern was obtained from UF_4 prepared by aqueous precipitation. Even pure UF_4 produces a relatively complicated pattern compared to UO_2.

pattern match	figure of merit	comment
UF_4	12.2	likely species
Corundum, Al_2O_3	18.2	standard used for 2θ calibration
Aluminum Oxide, Al_2O_3	39.8	likely from corundum standard

Table 5.7 – *X-ray Diffraction Pattern Match for Sample UF_4*: UF_4 and the corundum standard were the only likely species identified by x-ray diffraction.

Based on the x-ray diffraction pattern of the product (Figure 5.13), 4% hydrogen as a carrier gas appears to produce a mixture of UO_2 and UF_4 (Table 5.8), the actual ratio of which must be determined by chemical analysis. The most intense peak of UO_2 (measured at 2θ=28.2°) is clearly visible in the pattern, with the two next most intense peaks (46.95° and 55.7°) also appearing, but somewhat obscured by peaks from UF_4. Since the relative intensity of the 2θ=28.2° UO_2 signal is only 30.0% of the maximum intensity in the pattern, the less intense UO_2 peaks may be difficult to resolve from those of UF_4.

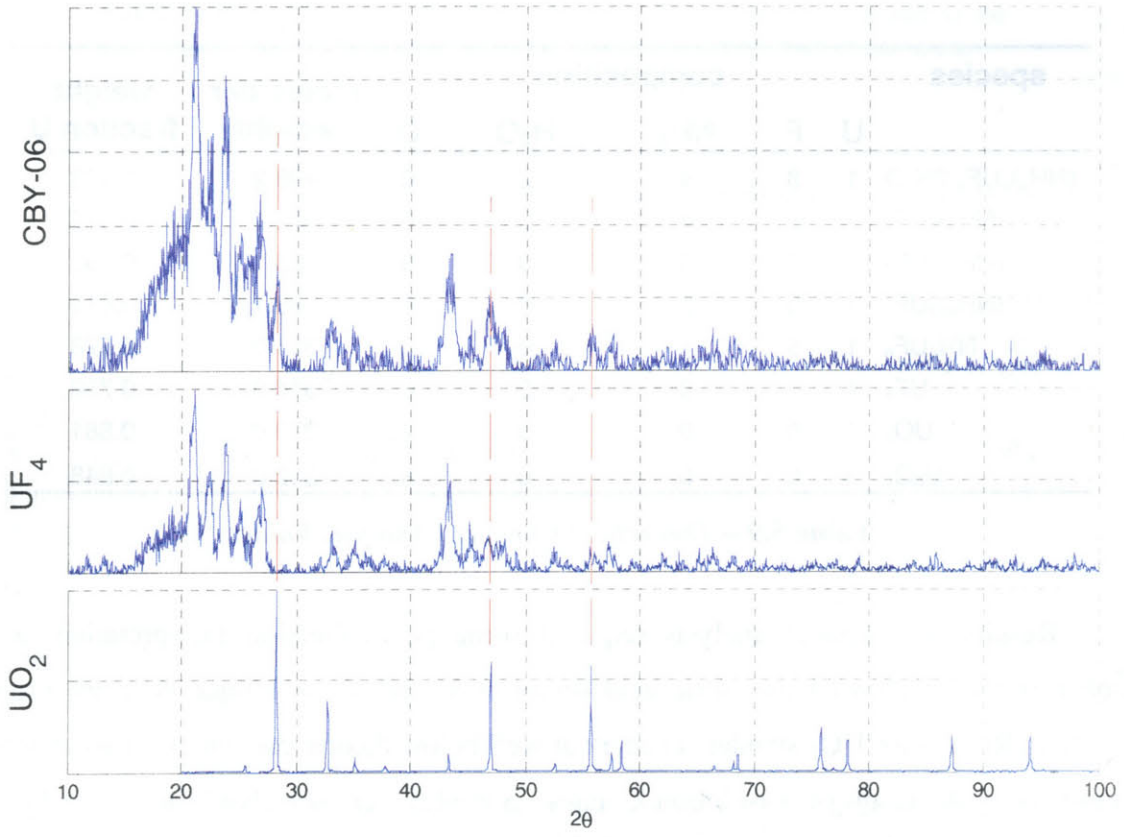

Figure 5.13 – *X-ray Diffraction Patterns of UO_2, UF_4, and Sample Prepared in 4% H_2*: The pattern most closely resembles UF_4, with the largest UO_2 peak also visible at 2θ=28.2º.

pattern match	figure of merit	comment
UF_4	16.8	likely species
Corundum, Al_2O_3	17.2	standard used for 2θ calibration
AlO(OH)	25.0	spurious match
UO_2	36.3	likely species
N_5H_5	40.5	spurious match
U_3O_7	42.7	possible, but no solid evidence
$UO_3 \cdot H_2O$	43.0	possible, but unlikely in H_2
Aluminum Oxide, Al_2O_3	44.0	likely from corundum standard
UO_3	44.2	possible, but unlikely in H_2
AlF_3	45.0	spurious match
$(NH_4)_2UF_6$	47.4	possible incomplete decomp.
$H_2U_3O_{10}$	49.8	possible, but unlikely in H_2

Table 5.8 – *Search Match List for Final Product Prepared in 4% Hydrogen*: UF_4, UO_2, and the corundum standard were the only likely species identified by x-ray diffraction. Small amounts of $(NH_4)_2UF_6$ may also be present, as well as NH_4UF_5, which may not have been identifiable by JADE.

Theoretical values for chemical analysis of compounds of interest are presented in Table 5.9.

species	composition					molecular weight	weight fraction U
	U	F	NH_4	H_2O	O		
$(NH_4)_4UF_8 \cdot 2H_2O$	1	8	4	2	0	498.2	0.478
$(NH_4)_4UF_8$	1	8	4	0	0	462.1	0.515
$(NH_4)_3UF_7$	1	7	3	0	0	425.1	0.560
$(NH_4)_2UF_6$	1	6	2	0	0	388.1	0.613
NH_4UF_5	1	5	1	0	0	351.0	0.678
UF_4	1	4	0	0	0	314.0	0.758
UO_2	1	0	0	0	2	270.0	0.881
U_3O_8	3	0	0	0	8	842.0	0.848

Table 5.9 – *Theoretical Chemical Analysis Values*

Results of chemical analysis required some post-collection interpretation, as the numbers returned showed the nitric acid dissolution analysis technique was not properly executed. Results for UO_2 standards came out well below theoretical values. This difference is most likely the result of dissolution kinetics. Samples were dissolved for a period of two days, but since the dissolution kinetics of uranium (IV) compounds are quite slow, even in

concentrated nitric acid, the dissolution may not have been complete. Given this, normalizing the data by using the known composition of the UO_2 standard was considered as a valid correction. Results are shown in Table 5.10. Results of the water dissolution are shown on Table 5.11.

sample	mass	U	gU/g	normalized
	mg	g/L		gU/g
CBY-lggcol-1	10.6	0.0177	0.335	0.521
CBY-bm-2	10.1	0.0163	0.323	0.504
CBY-01	11.7	0.0267	0.456	0.710
CBY-02a	11.6	0.0262	0.452	0.704
CBY-02b	14.0	0.0327	0.468	0.728
CBY-03	10.8	0.0258	0.478	0.745
CBY-05	11.3	0.0270	0.477	0.743
CBY-06	10.1	0.0255	0.504	0.785
CBY-04	14.6	0.0282	0.386	0.601
UO_2	15.7	0.0444	0.566	0.881
UF_4	10.0	0.0119*	0.476	0.742

*diluted to 50 mL

Table 5.10 – *Chemical Analysis Results*: Results are normalized to the theoretical value for UO_2 to account for incomplete dissolution of samples.

Figure 5.14 shows graphically the results of nitric acid dissolution chemical analysis.

Figure 5.14 – *Results of Nitric Acid Dissolution Analysis*: Blue dashed lines are drawn at uranium mass fraction values for the theoretical compounds. Points represent actual samples analyzed, normalized to the experimental value obtained for UO_2.

sample	mass mg	volume mL	[U] g/L	soluble gU/g
CBY-bm-2	24.0	25	0.092	0.096
CBY-01	16.0	25	0.095	0.149
CBY-02a	22.5	25	0.372	0.413
CBY-02b	20.2	25	0.184	0.227
CBY-03	25.5	25	0.309	0.303
CBY-05	27.6	25	0.361	0.327
CBY-06	24.9	25	0.225	0.226
CBY-04	25.3	25	0.168	0.166
UO2	51.4	25	0.007	0.003
UF4	33.5	25	0.100	0.075

Table 5.11 – *Results of Water Dissolution*: Uranium (VI) compounds formed are readily soluble in water. The most likely uranium (VI) compound is uranyl fluoride (UO_2F_2) and its associated ammonium fluoride double salts.

The data in Table 5.11 can be modified to account for the presence of uranium oxides and UF_4 in the final samples. By subtracting the concentration of soluble uranium obtained for the UF_4 standard, the contribution from other soluble uranium compounds can be obtained (Table 5.12 and Figure 5.15). Based on the assumption that UO_2 and U_3O_8 behave similarly in terms of water solubility and dissolution kinetics, the result for UO_2 can applied to samples in which U_3O_8 was a more likely species.

sample	soluble gU/g adjusted
CBY-01	0.071
CBY-02a	0.335
CBY-02b	0.149
CBY-03	0.225
CBY-05	0.249
CBY-06	0.148
CBY-04	0.088

Table 5.12 – *Adjusted Water Dissolution Results*: These values were adjusted to account for the dissolution of UF_4 and uranium oxides.

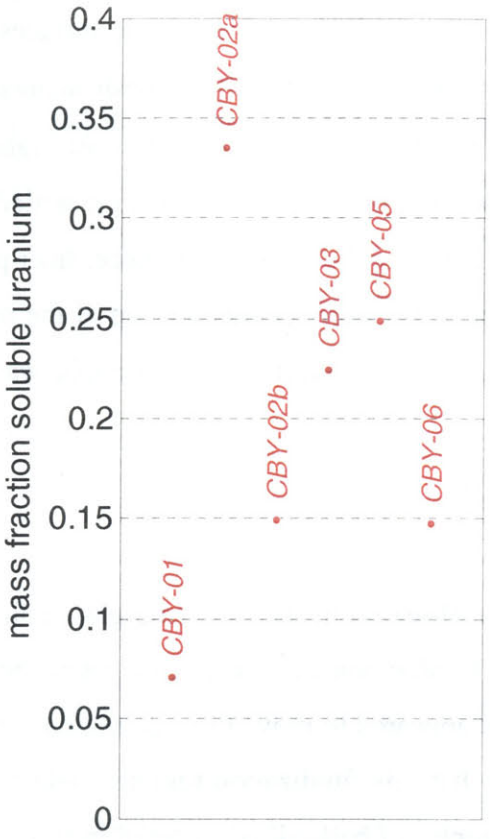

Figure 5.15 – *Results of Water Dissolution*: This plot shows values of soluble uranium mass fraction. Values have been adjusted by subtracting measured values for uranium tetrafluoride and uranium dioxide.

Dividing the adjusted soluble uranium content by the total uranium content gives the fraction of soluble uranium that cannot be attributed to uranium oxides or uranium tetrafluoride. Soluble uranium is most likely in the form of uranyl difluoride or partially decomposed ammonium uranyl fluoride double salts.

sample	soluble gU/g adjusted	normalized gU/g	not UF_4 or UO_x (likely uranyl difluoride)
CBY-01	0.071	0.710	9.96%
CBY-02a	0.335	0.704	47.53%
CBY-02b	0.149	0.728	20.50%
CBY-03	0.225	0.745	30.18%
CBY-05	0.249	0.743	33.50%
CBY-06	0.148	0.785	18.80%
CBY-04	0.088	0.601	14.63%

Table 5.13 – *Soluble Uranium not Attributable to Uranium Tetrafluoride or Uranium Oxides*

5.3 Materials Durability and Structural Integrity

Very little corrosion appeared on stainless steel surfaces within the column. Even after ten cycles at elevated temperatures, the 20μm mesh maintained its structural integrity, and was able to support the bed with no loss of material. At higher argon flows, much of the bed was carried into the upper part of the column, where it settled for lack of a particle arrest and return mechanism. By removing the top column piece, finer particles could be recovered. Larger conglomerations of particles were retained on top of the mesh in the lower part of the column. At lower argon flows, the majority of the sample was retained in the bed at the bottom of the column.

5.4 Bed Fluidization

Fluidization could be observed in the full-scale glass column at a variety of gas flow rates. Partial channelized fluidization at lower flow rates did not fully agitate the bed, although individual particles appeared to move through regions of fluidization. Based on this observation, it was decided that this fluidization regime could provide adequate agitation to the bed. After fluidizing samples of ball-milled material in this bed with argon for three days at 20 °C, the powder was light green in color, showing no visible signs of the darker-colored uranium oxides.

Chapter 6: Conclusions

6.1 Effectiveness of Ball Mill Technique for Fluorination

The larger particle size slowed the fluorination reaction by at least a factor of ten: from less then twenty minutes to on the order of one day; no difference in the fluorinated double salt products formed could be observed from X-ray diffraction (Figure 6.1).

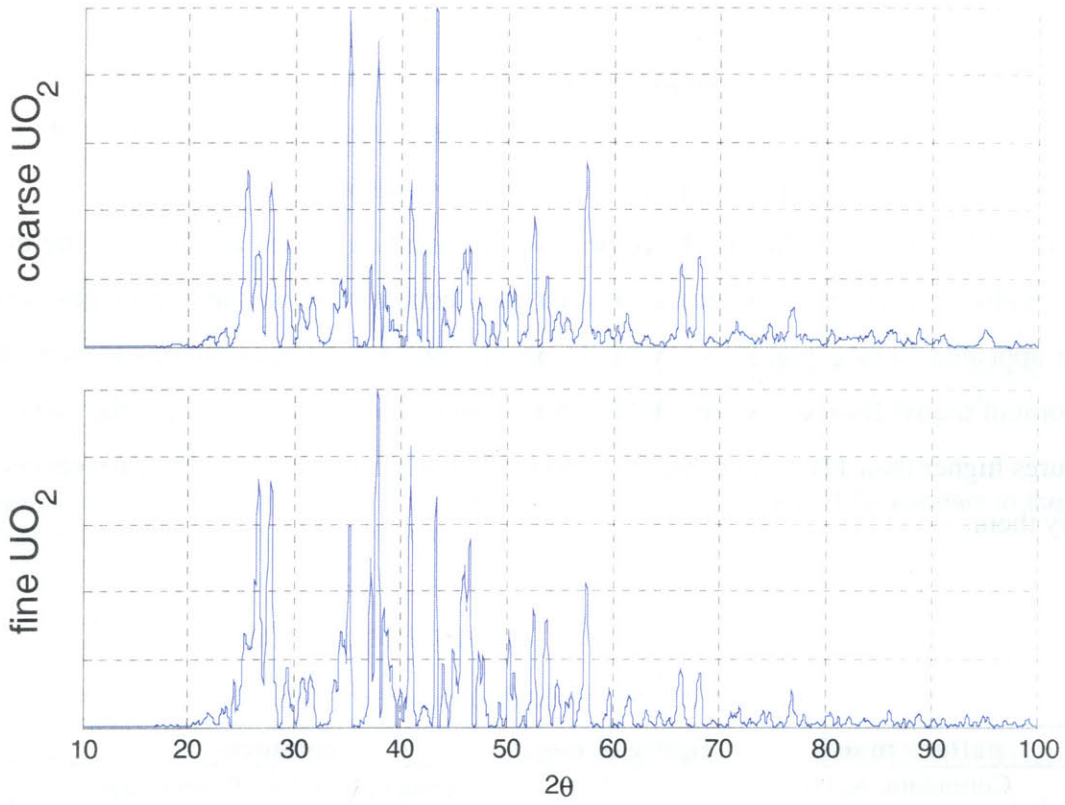

Figure 6.1 – *Samples Prepared from UO_2 with Different Particle Size*: These two samples are essentially the same, differing only by the amount of corundum standard.

Based on the visual color change and x-ray diffraction data, the ball mill appeared to be a viable method of preparing ammonium uranium fluoride double salts from uranium dioxide and ammonium bifluoride.

6.2 Effects of Plateau Temperatures

6.2.1 Lower Plateau Temperature

The lower plateau temperature effect can most easily be investigated in the stirred bed samples. In these, since the reactants were not finely ground, the lower plateau temperature was that at which the fluorination took place. At 80 °C, the fluorination reaction did not proceed sufficiently fast to complete the reaction in 4 hrs, but at 110 °C, the reaction was complete in 2.5 hours.

Trials with the ball milled reagents were less useful in determining what effect the lower hold temperature has on the overall process, only that the conditions used were sufficient to begin decomposition. The presence of U_3O_8 in the intermediate sample (Table 6.1 and Figure 6.2) indicates the reformation of uranium oxides at 110 °C. The most probable oxidizing agent was molecular oxygen as a contaminant in the carrier gas, since oxidation appeared to take place preferentially on the outside of larger clumps of particles. No ammonium uranyl fluorides were found in this sample, indicating that either they form at temperatures higher than 110 °C, or there was no sufficiently complete powder diffraction file to identify them.

pattern match	figure of merit	comment
Corundum, Al_2O_3	3.0	standard used for 2θ calibration
Aluminum Oxide, Al_2O_3	39.2	likely from corundum standard
U_3O_8	39.7	probable species
U_2N_3	45.2	possible, but unlikely to form
UN_2	46.1	from ammonia at 110 °C
$(NH_4)_2UF_6$	48.0	trace amounts

Table 6.1 – *Search Match List for Intermediate Product Sample*: U_3O_8 was identified in the sample, although the bulk of the sample was most likely $(NH_4)_4UF_8$ and $(NH_4)_3UF_7$, which would not have been identified by the JADE pattern match program.

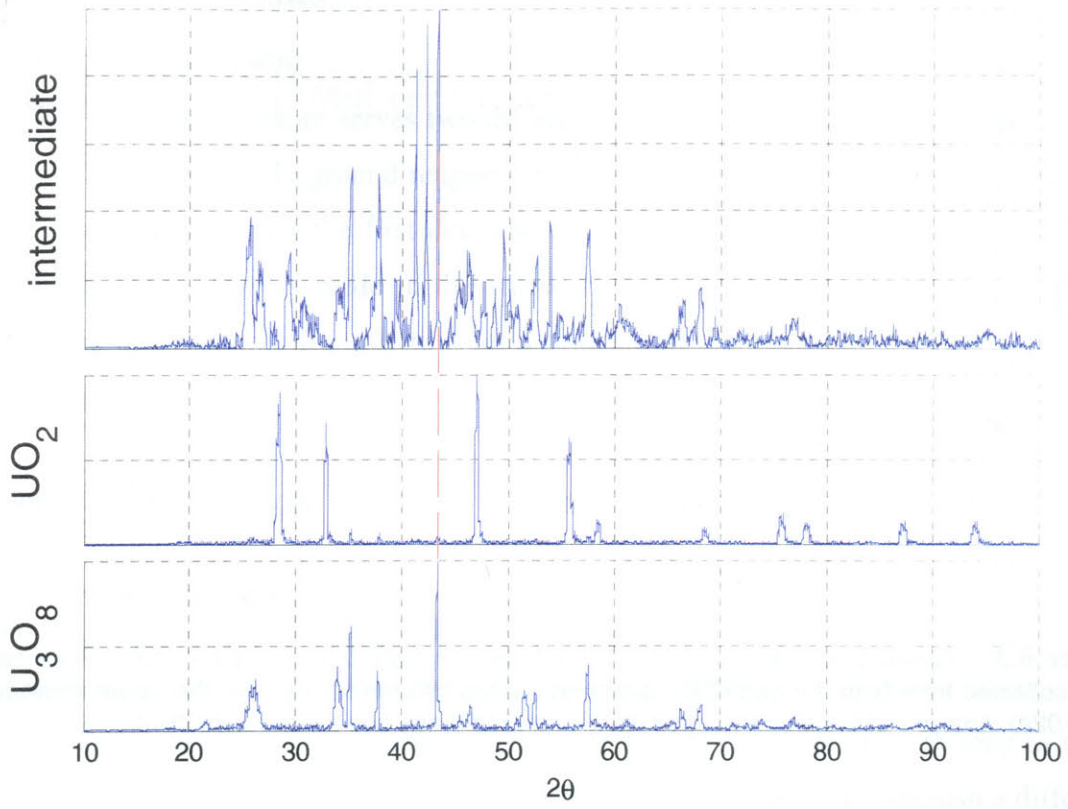

Figure 6.2 – *X-ray Diffraction Pattern of Intermediate Product*: U_3O_8 appears in the pattern of the intermediate product, which was removed after a hold at 110 °C.

6.2.2 Upper Plateau Temperature

Although not in the original experimental design, by looking at the difference between samples CBY-02a and CBY-02b, the decomposition temperature of $(NH_4)_2UF_6$ and $(NH_4)_2(UO_2)_2F_6{\cdot}3H_2O$ can be inferred. CBY-02a was removed from the top of the column, on the flange just below the outlet, while CBY-02b was removed from the bottom of the column on top of the mesh support. Since temperature was being measured in both locations (Figure 6.3) and conditions were otherwise identical, the presence and size of several low-2θ peaks (Figure 6.4) gave some hints as to the temperature speciation of the material in the column. $(NH_4)_2(UO_2)_2F_6{\cdot}3H_2O$ and $NH_4(UO_2)_2F_5{\cdot}3H_2O$ account for the larger peaks at 12° in the pattern of the sample from the top of the column. The presence of the 15° peak indicated a much larger fraction of $(NH_4)_2UF_6$ in the top of the column than in the bottom. Based on this, these compounds appear to decompose above 180 °C.

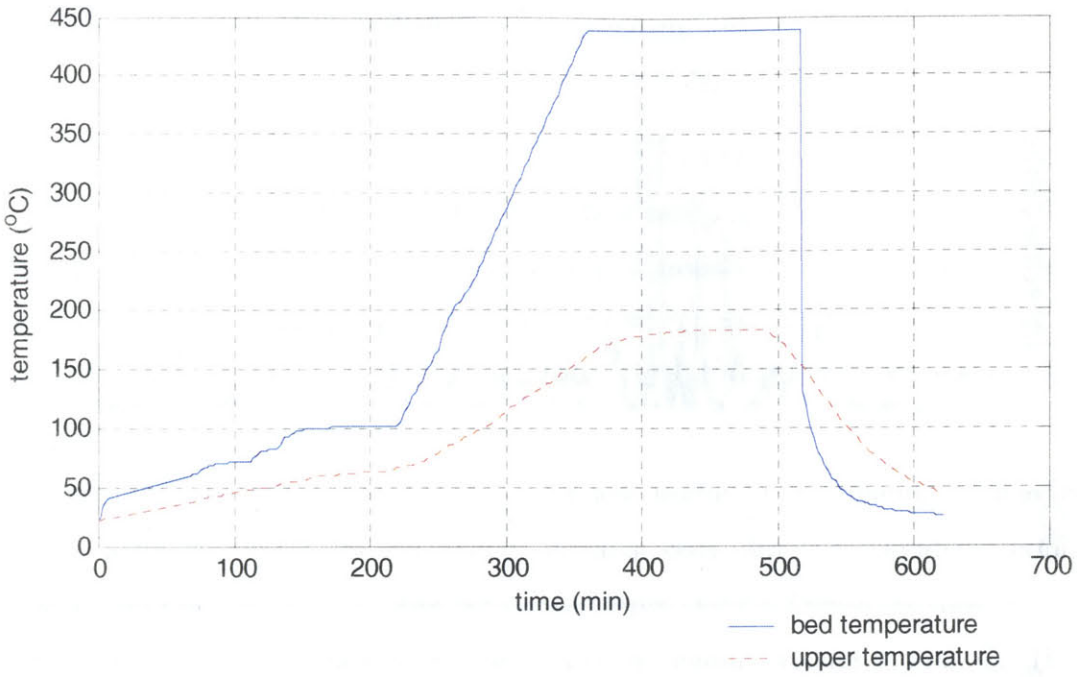

Figure 6.3 – *Temperature Measurements for Samples CBY-02a and CBY-02b*: Since samples were collected from both the bed (CBY-02b) and the top column flange near the upper thermocouple (CBY-02a), analysis of the samples essentially analyzed these two temperature cycles.

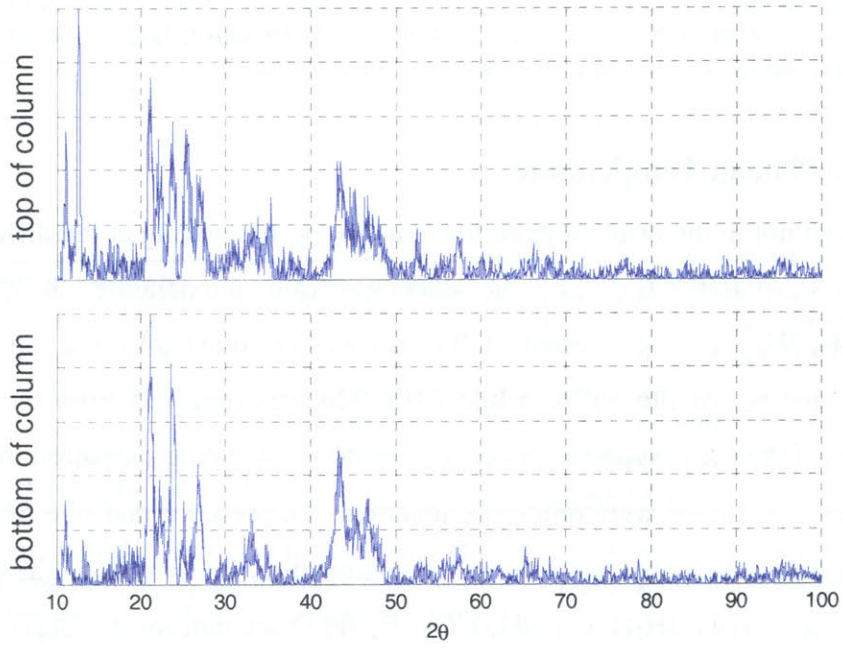

Figure 6.4 – *X-ray Diffraction Patterns of Samples CBY-02a and CBY-02b*: Except for decomposition temperature, conditions for these two samples were identical. The strong peaks from $(NH_4)_2(UO_2)_2F_6 \cdot 3H_2O$ and $NH_4(UO_2)_2F_5 \cdot 4H_2O$ are clearly visible in the top column samples, but is much less prevalent in the bottom sample.

6.3 Effects of Hold Times

6.3.1 Lower Hold Time

The lower temperature serves two different purposes depending on preparation of the reagents. The mechanically ground reagents were fully fluorinated, so the lower temperature plateau was solely to affect the first decomposition steps of the double salt. Based on the difference between samples made in the stirred bed, a hold time of at least three hours is necessary for ammonium bifluoride to fluorinate uranium dioxide when the reagents are still somewhat coarse.

6.3.2 Upper Hold Time

The final decomposition steps took place at temperatures near 425 °C. Based on analysis of samples CBY-03 and CBY-05, the upper hold time had little impact on the chemical composition of the final products. These samples were prepared under similar conditions, except that the overall temperature cycle for CBY-05 was twice as long as that of CBY-03. Given this, since both chemical and XRD analysis failed to distinguish a difference between the samples, any partially decomposed double salt remaining in the sample is more likely attributable to plateau temperature, not hold time.

6.4 Effects of carrier gas

Samples CBY-05 and CBY-06 were prepared under similar conditions, except carrier gas. CBY-06, prepared in 4% hydrogen in argon, had 15% less soluble uranium than CBY-05, as well as showing no traces of uranyl difluoride or its associated double salts in its XRD pattern.

A reducing environment is necessary to avoid the formation of uranyl difluoride and U_3O_8 impurities. Depending on the subsequent use of the product UF_4, this may or may not be important. If UF_4 is being made as feedstock for a Fluorox process, UO_2F_2 is an unimportant impurity as it is a product of the Fluorox process anyway, and the subsequent separation of UF_6 from UO_2F_2 is easily accomplished utilizing the high volatility of UF_6. In this case, it would not be necessary to maintain reducing conditions during the fluorination and decomposition process.

If UF_4 is being made to use in a calcium reduction of UF_4 to uranium metal, any oxygen impurities will react highly exothermically with calcium metal, making it difficult to maintain the physical integrity of the reacting UF_4 and calcium metal. Instead of obtaining an ingot of uranium metal topped with calcium fluoride slag, the heat of reaction with oxygen compounds tends to disperse the uranium metal. For this application, a reducing environment would lower the overall oxygen content of the UF_4, thus making it better suited for calcium reduction.

6.5 Suitability of Construction Materials

Based on visual inspection of the stainless steel fluidized bed apparatus, stainless steel is a suitable material of construction for this type of process equipment. Even the bed-supporting mesh, with its high surface area, was not corroded by the reagents and temperatures used. In the stirred bed trials, mild steel components corroded quickly, reducing their functionality as mechanical parts and likely adding iron oxide as an impurity to the material in the bed.

6.6 Fluidized Bed versus Stirred Bed

6.6.1 Advantages of the Stirred Bed

With the stirred bed, it was not necessary to preheat the incoming gas stream, as the flow was low enough to allow the temperature to be controlled in the bed without necessitating preheating of the inlet gas. As the extensive amount of copper tubing used in the preheater was a likely source of oxygen contamination in the fluidized bed apparatus, the lack of a preheater is a significant simplification that eliminates this problem. Oxygen impurity levels were most likely lower in the stirred bed than the fluidized bed.

6.6.2 Advantages of the Fluidized Bed

The fluidized bed is a much simpler mechanical device, and this advantage became apparent in the difficulty in fully mixing the stirred bed. In an attempt to fully mix the vessel, mild steel shimstock attached to the paddle corroded and was only marginally effective in closing the gap between the paddle and crucible wall.

Even with a lower flow rate than is needed for full fluidization, channelized fluidization provided adequate mixing. With the variation in particle size inherent in commercial UO_2, it would be impractical to specify a particle size consistent enough to design a fluidized bed with a particle arresting and return system, as was absent in this fluidized bed apparatus. A tapered shim to cover the flat flange at the top of the column could serve as a rudimentary particle return system, thus allowing for fluidization with less loss of material. In addition, oxygen impurity levels could be lowered by installing an oxygen getter near the inlet to the bed.

THIS PAGE INTENTIONALLY LEFT BLANK

References

[1] Van Impe J, Chemical Engineering Progress, **50** #5 (May, 1954), 230-234.

[2] Quil B, "Spill Prevention Guidance Document," Naval Facilities Engineering Service Center, UG-2033-ENV, Appendix E, October, 1998.

[3] Decroly C and Van Impe J, Belgian Patent 500558, July 11, 1951.

[4] Galkin NP, Sudarikov BN, et. al., Technology of Uranium, translated from Russian by USAEC, Springfield, Va : available from the U.S. Dept. of Commerce, Clearinghouse for Federal Scientific and Technical Information, 1966, p 28.

[5] DOE/EIS-0269 "Final Programmatic Environmental Impact Statement for Alternative Strategies for the Long Term Management and Use of Depleted Uranium Hexafluoride," Appendix A.

[6] Cordfunke EHP, The Chemistry of Uranium, Amsterdam: Elsevier Publishing, 1969, pp. 128-129.

[7] Wani BN, Patwe SJ, et. al., Journal of Fluorine Chemistry, **44** (1989), 177-185.

[8] Euler RD and Westrum EF Jr., Journal of Physical Chemistry, **65** (1961), 1291-1296.

[9] Wani BN, Patwe SJ, et. al., Journal of Fluorine Chemistry, **44** (1989), 177-185.

[10] Benz R, Douglass RM, et. al., Inorganic Chemistry, **2** #4 (1963), 799-803.

11 Yahata T, Muromura T, et.at., Journal of Inorganic Nuclear Chemistry, 33 (1971), 3339-3343.

[12] Penneman RA, Kruse FH, et. al., Inorganic Chemistry, **3** #3 (1964), 309-315.

[13] Galkin NP, Sudarikov BN, and Zaitsev VA, Atomnaya Énergiya, **11** #6 (1961), 554-555.

[14] Wani BN and Rao URK, Materials Chemistry and Physics, **33** (1993), 165-167.

[15] Bhide MK, Page AG, et. al., *Source Unknown*, Bhabha Atomic Research Centre, Trombay, Bomby-85.

[16] Decroly C and Van Impe J, Belgian Patent 496487, July 15, 1950.

17 Ellis AS and Mooney RB, US Patent 2650153, August 25, 1953.

[18] Sanlaville J, Preparation of Uranium Tetrafluoride from UO_3 or Uranyl Salt, P/1259 France.

[19] Tolley WB, HW-35814 (1955).

[20] Robinson RE, Geertsma JC, and Paynter JC, P/464 South Africa 264.

[21] Leah (Ellis) AS and Mooney RB, US Patent 2654654, October 6, 1953.

[22] Galkin NP, Sudarikov BN, et. al., Technology of Uranium, translated from Russian by USAEC, Springfield, Va : available from the U. S. Dept. of Commerce, Clearinghouse for Federal Scientific and Technical Information, 1966, p 296.

[23] Geertsma JC, Hart HP, et. al., Thermal Decomposition of Ammonium Uranous Fluoride to Uranium Tetrafluoride in a Fluidized Bed Reactor: Progress Report on Experimental Work on a 30-inch Diameter Fluidized-Bed Reactor, Atomic Energy Board, PEL 121 South Africa, 1965.

[24] Grace JR, Canadian Journal of Chemical Engineering, **64** (1986), 353-363.

[25] Geldart D, Powder Technology, **7** (1973), 285-292.

[26] McCabe WL, Smith JC, Harriott P, Unit Operations of Chemical Engineering, Sixth Edition, Boston: McGraw-Hill, 2001, p.173.

[27] Pell M and Dunson JB, Section 17 from Perry's Chemical Engineers' Handbook, Seventh Edition, ed. Perry RH and Green DW, New York: McGraw-Hill, 1997.

Appendix A – Engineering Drawings for Stainless Steel Column

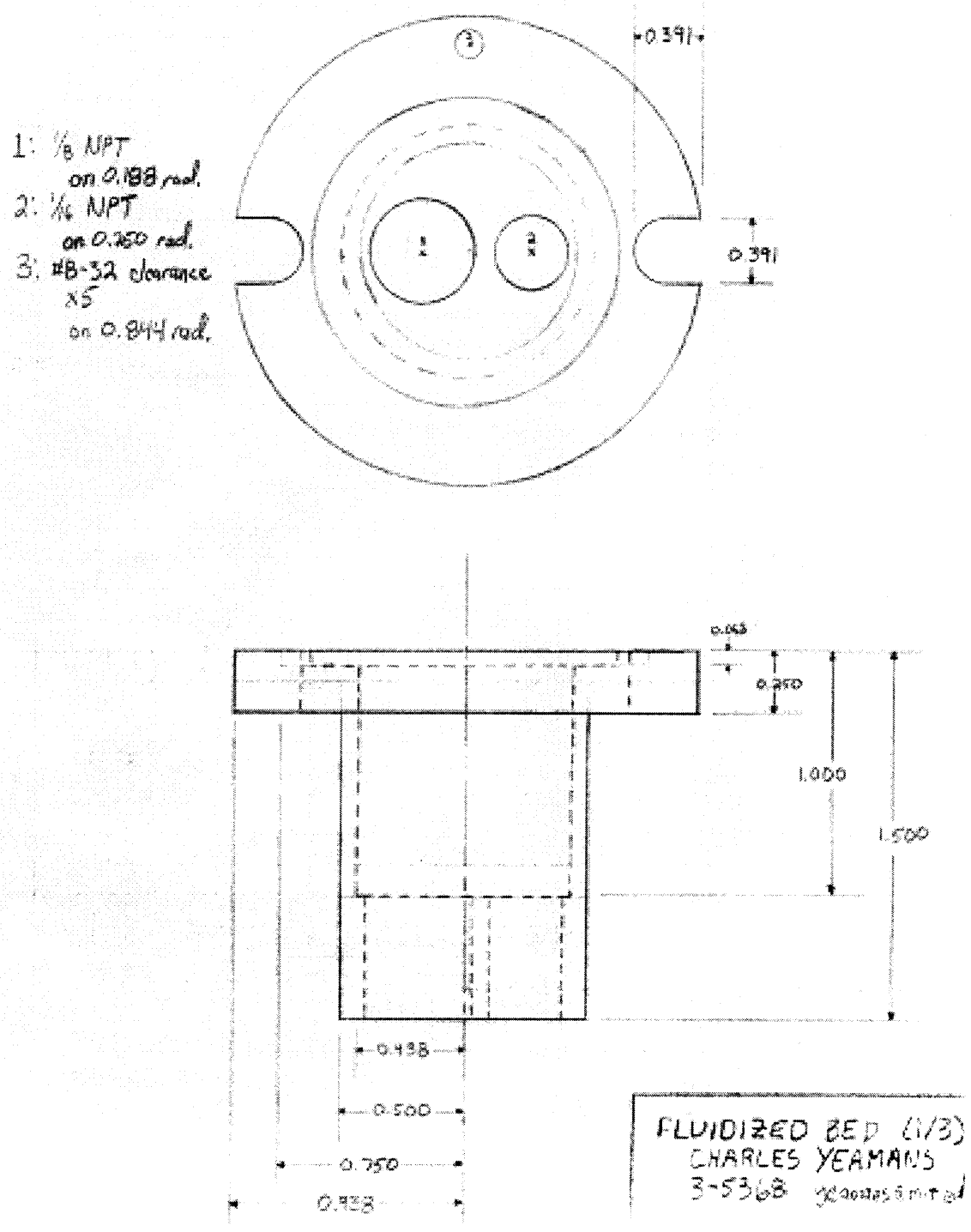

Figure A.1 – *Bottom Column Part*: The bed is supported on the top flange, which mates to the bottom of Part 2.

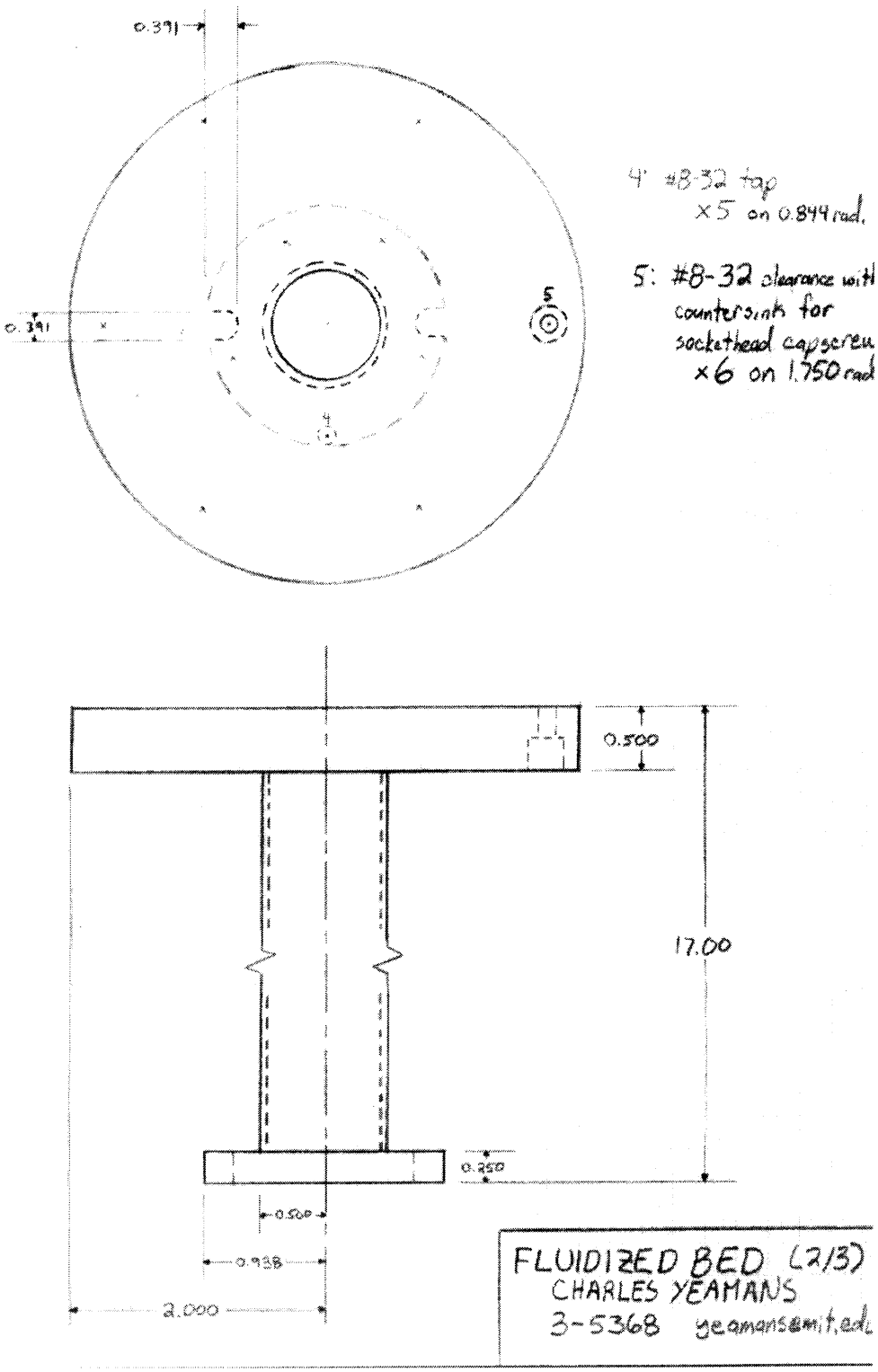

Figure A.2 – *Middle Column Part*

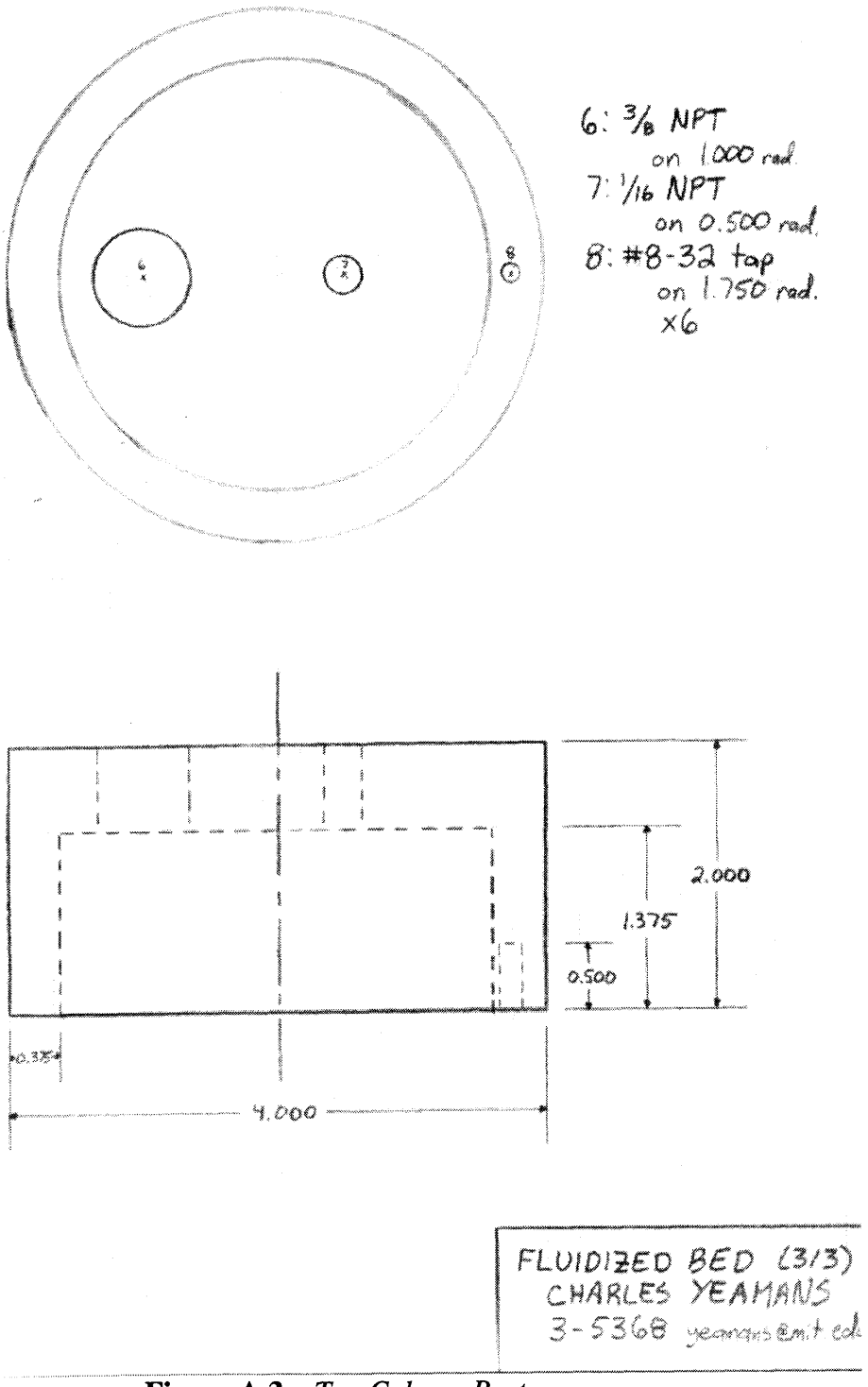

Figure A.3 – *Top Column Part*

THIS PAGE UNINTENTIONALLY LEFT BLANK

Appendix B X-ray Diffraction Patterns and Search Match Lists

[Z13957.RAW] ~~MYSTERY POWDER~~ UO_2 S/M Hit Listing

SCAN: 20.0/100.0/0.05/1(sec), Cu, I(max)=21498, 05/26/03 15:50

NOTE: Intensity = Counts, 2T(0)=0.0(°), S/M: Default Search_Match (Use Chemistry Filter)

J-Column: [+] Common/Good Patterns, [?] Uncommon/Non-Ambient Patterns, [ ] Intermediate Patterns, [D] Deleted

D-Column: C=Calculated, D=Diffractometer, F=Densitometer, V=Film/Visual, X=Other/Unknown

#	40 Hits Sorted on Figure-Of-Merit	FOM	I%	2T(0)	d/d(0)	PDF-#	J	D	Density
1	Uraninite, syn - UO2	1.7	88	0.000	1.000	65-0285	?	C	10.953
2	Corundum, syn - Al2O3	6.0	7	0.000	1.000	10-0173	+	D	4.050

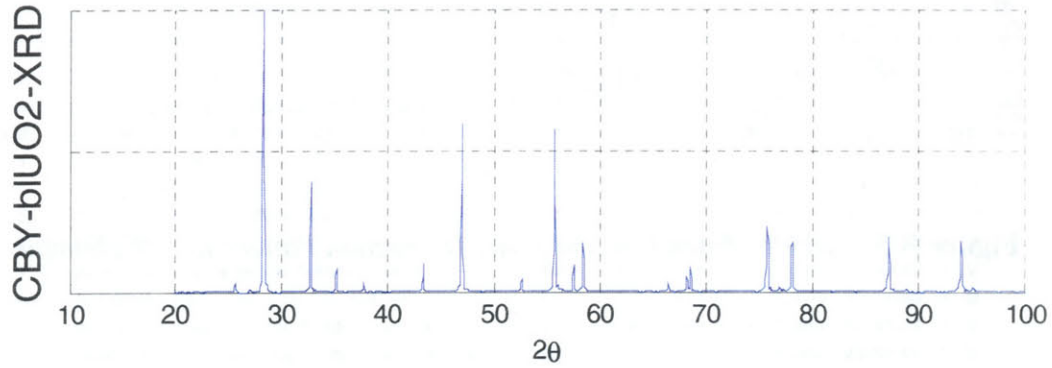

Figure B.1 – *Search Match List and X-ray Diffraction Pattern for UO_2 Sample*

[Z14757.RAW] U3O8 S/M Hit Listing

SCAN: 10.0/100.0/0.01/1.75(sec), Cu, I(max)=5799, 07/23/03 22:16

NOTE: Intensity = Counts, 2T(0)=0.0(°), S/M: Default Search_Match (Use Chemistry Filter)

J-Column: [+] Common/Good Patterns, [?] Uncommon/Non-Ambient Patterns, [ ] Intermediate Pat...

D-Column: C=Calculated, D=Diffractometer, F=Densitometer, V=Film/Visual, X=Other/Unknown

#	40 Hits Sorted on Figure-Of-Merit	FOM	I%	2T(0)	d/d(0)	PDF-#	J	D
1	Corundum, syn - Al2O3	4.7	76	0.000	1.000	10-0173	+	D
2	U3O8 - Uranium Oxide	10.9	23	0.000	1.000	47-1493	?	D
3	U3O8 - Uranium Oxide	13.8	27	0.000	1.000	31-1425	?	C
4	UO3 - Uranium Oxide	26.1	27	0.120	1.000	31-1416	?	C

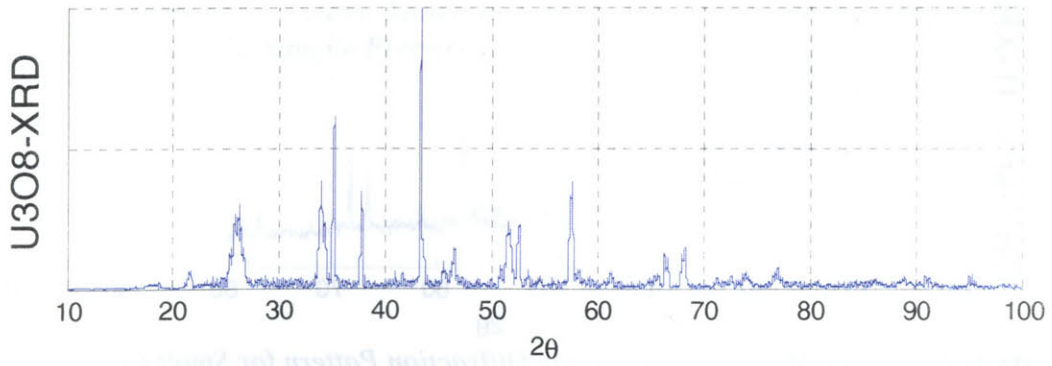

Figure B.2 – *Search Match List and X-ray Diffraction Pattern for U_3O_8 Sample*

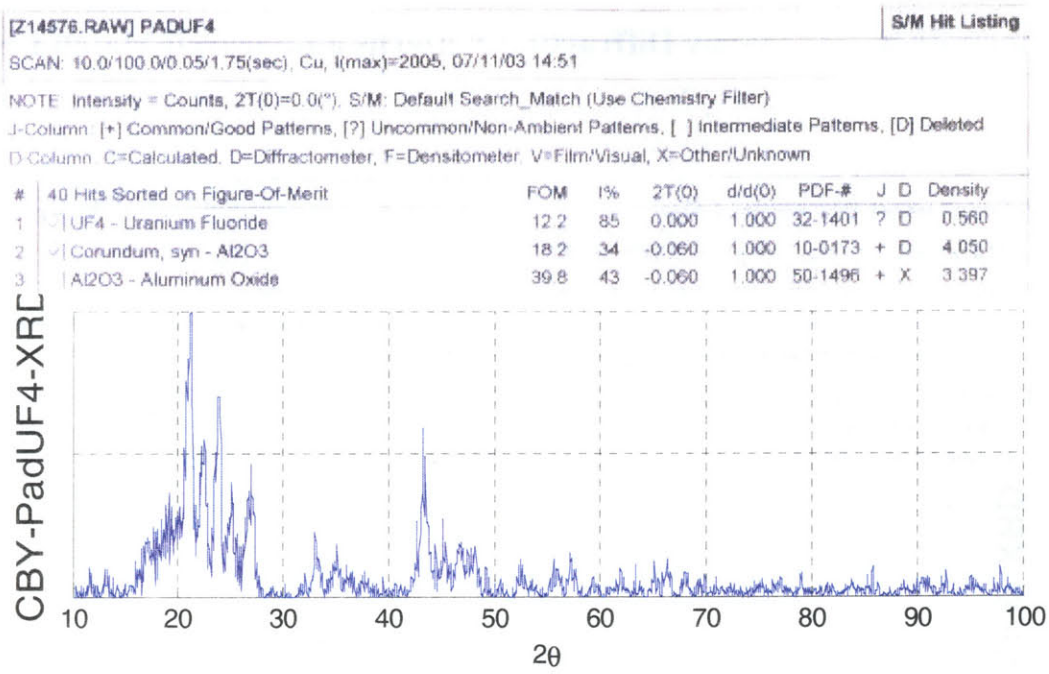

Figure B.3 – Search *Match List and X-ray Diffraction Pattern for UF_4 Sample*

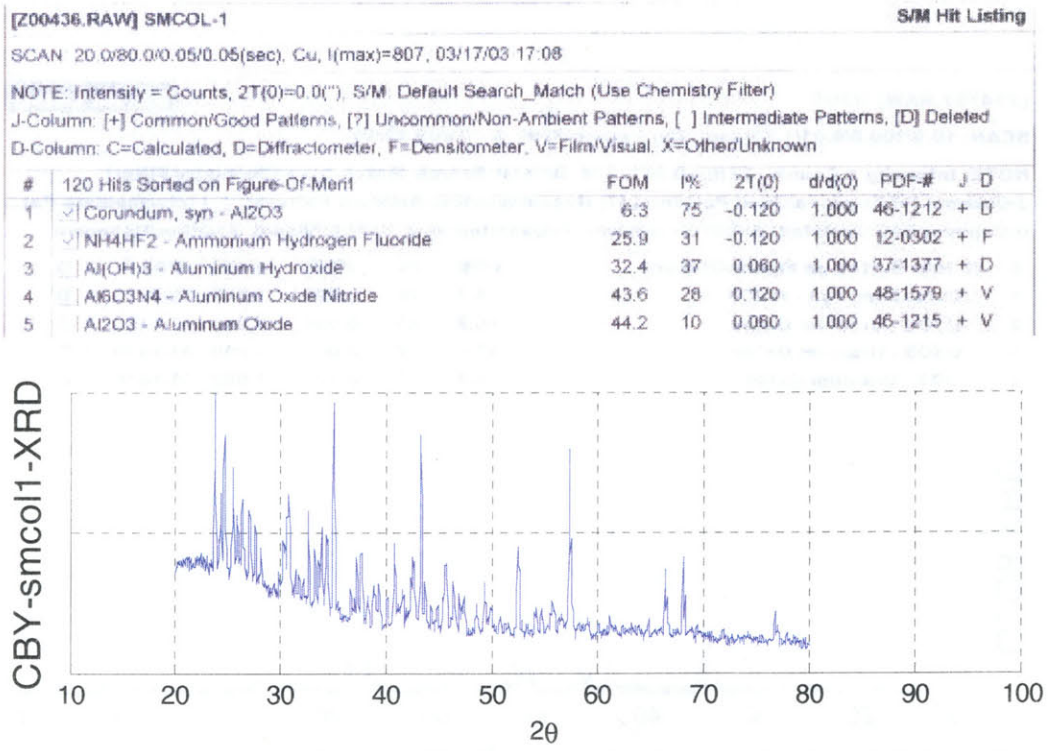

Figure B.4 – *Search Match List and X-ray Diffraction Pattern for Small Column Sample*

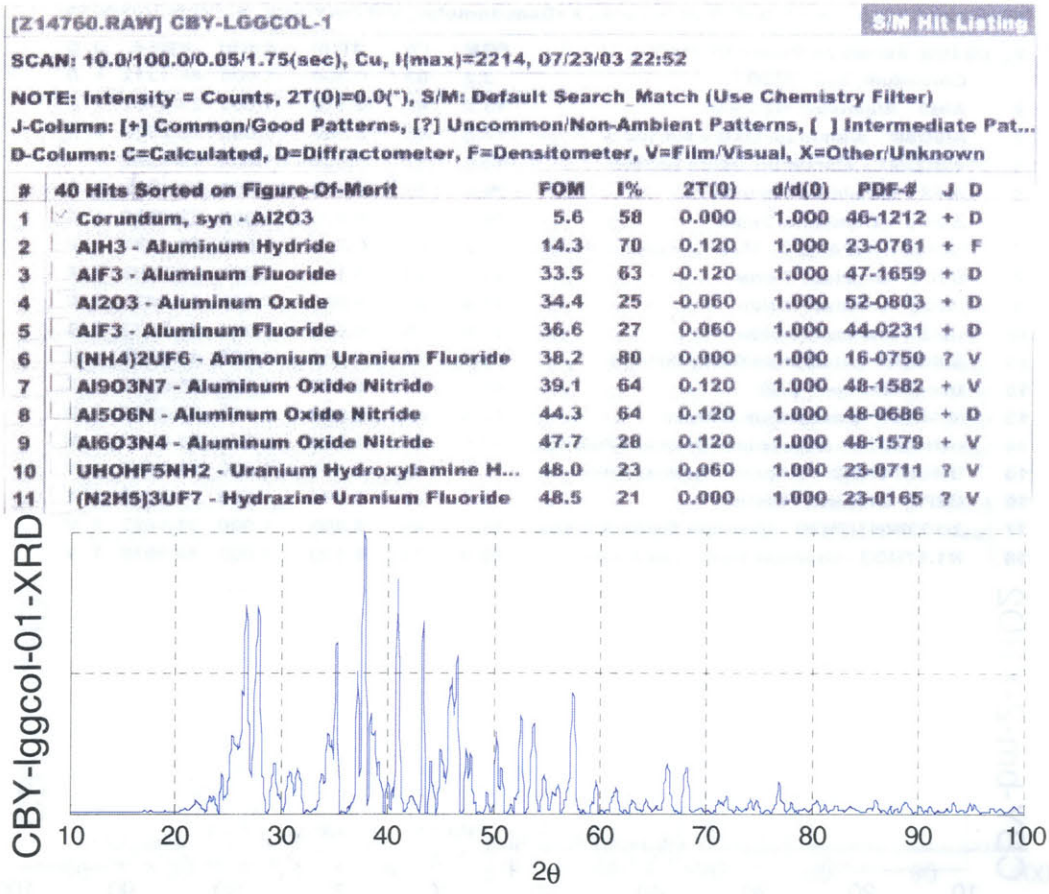

Figure B.5 – *Search Match List and X-ray Diffraction Pattern for Ball-Milled Sample Prepared from Coarse UO_2*

[Z14761.RAW] CBY-BM-2 S/M Hit Listing

SCAN: 10.0/100.0/0.05/1.75(sec), Cu, I(max)=2451, 07/23/03 23:04

NOTE: Intensity = Counts, 2T(0)=0.0(°), S/M: Default Search_Match (Use Chemistry Filter)

J-Column: [+] Common/Good Patterns, [?] Uncommon/Non-Ambient Patterns, [ ] Intermediate Pat...

D-Column: C=Calculated, D=Diffractometer, F=Densitometer, V=Film/Visual, X=Other/Unknown

#	40 Hits Sorted on Figure-Of-Merit	FOM	I%	2T(0)	d/d(0)	PDF-#	J	D
1	Corundum, syn - Al2O3	3.2	83	0.000	1.000	46-1212	+	D
2	AlH3 - Aluminum Hydride	13.2	47	0.120	1.000	23-0761	+	F
3	Al5O6N - Aluminum Oxide Nitride	17.5	47	0.060	1.000	48-0686	+	D
4	Al9O3N7 - Aluminum Oxide Nitride	18.6	47	0.060	1.000	48-1582	+	V
5	AlF3 - Aluminum Fluoride	26.6	38	0.060	1.000	47-1659	+	D
6	Al2O3 - Aluminum Oxide	28.5	46	0.120	1.000	52-0803	+	D
7	(NH3OH)AlF4!H2O - Hydroxylammonium f...	31.2	21	0.000	1.000	46-1086	?	V
8	U2O5 - Uranium Oxide	31.3	28	0.120	1.000	10-0099	?	X
9	U3O8 - Uranium Oxide	31.4	23	0.060	1.000	31-1425	?	C
10	UN2 - Uranium Nitride	36.9	25	0.060	1.000	65-2973	?	C
11	Al6O3N4 - Aluminum Oxide Nitride	39.8	18	0.060	1.000	48-1579	+	V
12	Uraninite, syn - UO2	41.6	47	-0.060	1.000	65-0286	?	C
13	NH4NO3 - Ammonium Nitrate	42.3	46	0.060	1.000	47-0866	?	D
14	(NH4)2UF6 - Ammonium Uranium Fluoride	43.5	31	0.000	1.000	16-0750	?	V
15	UHOHF5NH2 - Uranium Hydroxylamine H...	43.7	49	-0.120	1.000	23-0711	?	V
16	U2F9 - Uranium Fluoride	45.2	20	-0.060	1.000	04-0860	?	X
17	2UO3!NH3!3H2O - Uranium Oxide Ammon...	48.0	46	0.000	1.000	31-1427	?	V
18	H1.17UO3 - Uranium Hydrogen Oxide	48.9	23	0.120	1.000	38-0039	?	V

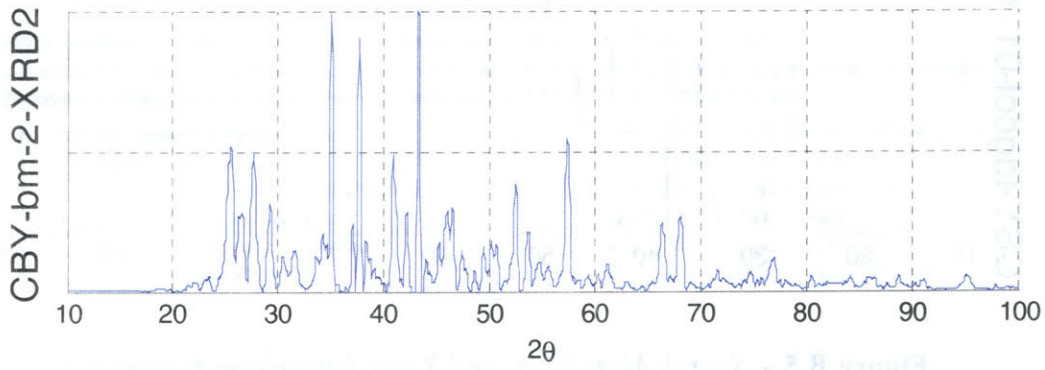

Figure B.6 – *Search Match List and X-ray Diffraction Pattern for Ball-Milled Sample Prepared from Fine UO_2*

[Z14577.RAW] CBY-01 S/M Hit Listing

SCAN: 10.0/100.0/0.05/1.75(sec), Cu, I(max)=2720, 07/11/03 15:02

NOTE: Intensity = Counts, 2T(0)=0.0(°), S/M: Default Search_Match (Use Chemistry Filter)

J-Column: [+] Common/Good Patterns, [?] Uncommon/Non-Ambient Patterns, [ ] Intermediate Patterns, [D] Deleted

D-Column: C=Calculated, D=Diffractometer, F=Densitometer, V=Film/Visual, X=Other/Unknown

#	80 Hits Sorted on Figure-Of-Merit	FOM	I%	2T(0)	d/d(0)	PDF-#	J	D	Density
1	Al2O3 - Aluminum Oxide	12.7	15	-0.060	1.000	50-1496	+	X	3.397
2	Unnamed mineral [NR] - UO3-H2O	20.9	15	-0.060	1.000	15-0569	?	X	
3	(NH4)(UO2)2F5!4H2O - Ammonium Uranyl Fluorid	24.5	74	0.060	1.000	26-0095	?	D	4.130
4	Corundum, syn - Al2O3	25.6	14	0.060	1.000	10-0173	+	D	4.050
5	(NH4)2(UO2)2F5!3H2O - Ammonium Uranyl Fluor	29.9	15	-0.060	1.000	25-0046	?	D	4.280
6	UF4 - Uranium Fluoride	33.8	23	0.060	1.000	32-1401	?	D	0.560
7	(NH3OH)AlF4!H2O - Hydroxylammonium fluoroalu	44.2	25	0.120	1.000	46-1086	?	V	0.403
8	UO2(OH)2 - Uranyl Hydroxide	44.2	7	0.000	1.000	30-1403	?	X	5.820
9	N2H4UF4 - Uranium Fluoride Hydrazine	45.0	15	0.000	1.000	28-1404	?	V	
10	AlF3 - Aluminum Fluoride	48.9	3	0.000	1.000	43-0435	+	V	2.815
11	Diaspore - AlO(OH)	49.4	18	-0.060	1.000	05-0355	+	D	3.440

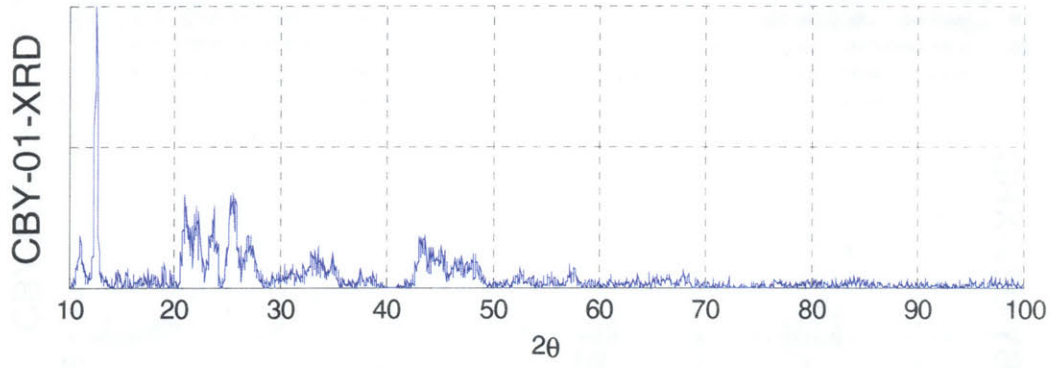

Figure B.7 – *Search Match List and X-ray Diffraction Pattern for Sample CBY-01*

[Z14578.RAW] CBY-02A | S/M Hit Listing

SCAN: 10.0/100.0/0.05/1.75(sec), Cu, I(max)=1196, 07/11/03 15:11

NOTE: Intensity = Counts, 2T(0)=0.0(°), S/M: Default Search_Match (Use Chemistry Filter)
J-Column: [*] Common/Good Patterns, [?] Uncommon/Non-Ambient Patterns, [ ] Intermediate Patterns, [D] Deleted
D-Column: C=Calculated, D=Diffractometer, F=Densitometer, V=Film/Visual, X=Other/Unknown

#	40 Hits Sorted on Figure-Of-Merit	FOM	I%	2T(0)	d/d(0)	PDF-#	J	D	Density
1	(NH4)(UO2)2F5I4H2O - Ammonium Uranyl Fluorid	13.6	86	0.060	1.000	26-0095	?	D	4.130
2	Unnamed mineral [NR] - UO3-H2O	15.0	40	-0.120	1.000	51-1483	?	D	
3	UF4 - Uranium Fluoride	15.2	56	0.000	1.000	32-1401	?	D	0.560
4	UO2(OH)2 - Uranyl Hydroxide	18.8	23	-0.060	1.000	30-1403	?	X	5.820
5	(NH4)2(UO2)2F5I3H2O - Ammonium Uranyl Fluor	20.0	40	-0.060	1.000	25-0046	?	D	4.280
6	Corundum, syn - Al2O3	21.0	34	0.000	1.000	10-0173	+	D	4.050
7	Diaspore - AlO(OH)	30.1	33	0.000	1.000	05-0355	+	D	3.440
8	H2U3O10 - Hydrogen Uranium Oxide	30.2	62	0.060	1.000	27-0201	?	C	6.851
9	N5H5 - Hydrazine Azide	30.8	30	-0.060	1.000	26-0751	+	V	1.400
10	UO2F2'1.5H2O - Uranyl Fluoride Hydrate	32.1	57	0.060	1.000	24-1154	?	V	4.720
11	N2H4UF4 - Uranium Fluoride Hydrazine	33.5	28	-0.120	1.000	28-1404	?	V	
12	Al2O3 - Aluminum Oxide	33.6	56	0.120	1.000	31-0026		D	
13	(NH3OH)AlF4!H2O - Hydroxylammonium fluoroalu	36.1	67	0.060	1.000	46-1086	?	V	0.403
14	UO2.87 - Uranium Oxide	37.1	68	0.120	1.000	46-0949	?	X	11.342
15	(NH4)x+2(PxO3x+1) - Ammonium polyphosphate	41.7	11	-0.060	1.000	44-0739	?	X	
16	UO3 - Uranium Oxide	44.4	10	-0.060	1.000	46-0952	?	X	11.351
17	AlF3 - Aluminum Fluoride	45.0	7	-0.060	1.000	43-0435	+	V	2.815
18	UO2F2'2H2O - Uranyl Fluoride Hydrate	45.5	43	0.120	1.000	47-0577	?	D	0.201
19	Ianthinite - U6O7(OH)20	45.5	9	-0.060	1.000	12-0272	?	V	5.160
20	(UF5(NH3)OH) - Uranium Ammine Fluoride Hydrox	45.6	12	-0.060	1.000	17-0287	?	V	
21	Al(NO3)3!9H2O - Aluminum Nitrate Hydrate	46.1	31	-0.060	1.000	01-0435		X	
22	U3O8 - Uranium Oxide	46.0	41	-0.060	1.000	43-1419	?	V	15.900

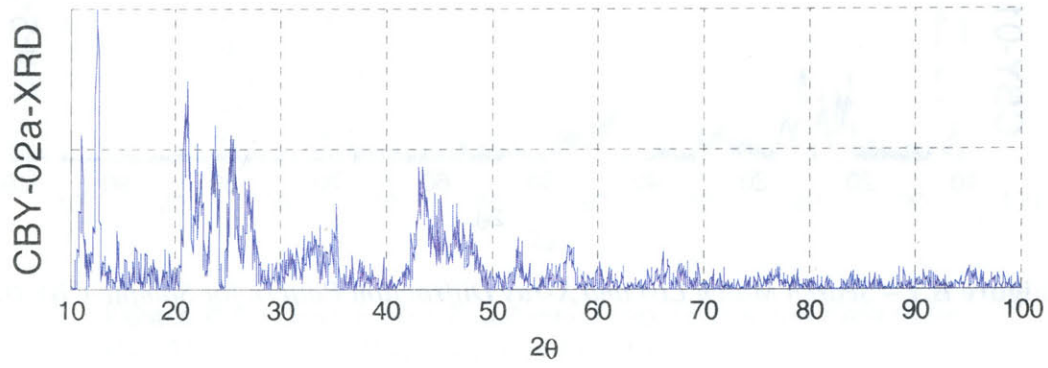

Figure B.8 – *Search Match List and X-ray Diffraction Pattern for Sample CBY-02a*: This sample was removed from the top flange of the column.

[Z14579.RAW] CBY-02B | S/M Hit Listing

SCAN: 10.0/100.0/0.05/1.75(sec), Cu, I(max)=1356, 07/11/03 15:22

NOTE: Intensity = Counts, 2T(0)=0.0(°), S/M: Default Search_Match (Use Chemistry Filter)
J-Column: [+] Common/Good Patterns, [?] Uncommon/Non-Ambient Patterns, [ ] Intermediate Patterns, [D] Deleted
D-Column: C=Calculated, D=Diffractometer, F=Densitometer, V=Film/Visual, X=Other/Unknown

#	40 Hits Sorted on Figure-Of-Merit	FOM	I%	2T(0)	d/d(0)	PDF-#	J	D	Density
1	[✓] UF4 - Uranium Fluoride	14.6	73	0.120	1.000	12-0701	?	V	6.559
2	[✓] Corundum, syn - Al2O3	24.0	43	-0.060	1.000	10-0173	+	D	4.050
3	[ ] Diaspore - AlO(OH)	25.2	25	0.060	1.000	05-0355	+	D	3.440
4	[✓] Unnamed mineral [NR] - UO3-H2O	29.2	25	-0.060	1.000	15-0569	?	X	
5	[ ] AlF3 - Aluminum Fluoride	32.5	20	0.000	1.000	43-0435	+	V	2.815
6	[ ] UO3 - Uranium Oxide	34.5	43	-0.060	1.000	18-1429	?	V	8.540
7	[ ] Ianthinite - U6O7(OH)20	35.7	7	0.060	1.000	12-0272	?	V	5.160
8	[ ] UO3!zNH3!xH2O - Ammonia Uranium Oxide Hydr...	37.1	10	0.060	1.000	14-0340	?	V	
9	[ ] UO2(OH)2 - Uranyl Hydroxide	38.2	18	-0.120	1.000	30-1403	?	X	5.820
10	[ ] Al2O3 - Aluminum Oxide	38.5	34	0.000	1.000	50-1496	+	X	3.397
11	[ ] N5H5 - Hydrazine Azide	42.2	25	0.000	1.000	26-0751	+	V	1.400
12	[ ] (NH4)2(UO2)2F5!3H2O - Ammonium Uranyl Fluor...	42.4	23	-0.060	1.000	25-0046	?	D	4.280
13	[ ] H2O - Ice	43.6	9	0.060	1.000	16-0665	?	V	1.196
14	[ ] NH4HF2 - Ammonium Hydrogen Fluoride	45.2	12	0.060	1.000	12-0302	+	F	1.499
15	[ ] H2U3O10 - Hydrogen Uranium Oxide	48.9	72	-0.060	1.000	27-0201	?	C	6.851
16	[ ] U3O8 - Uranium Oxide	49.3	61	-0.120	1.000	20-1345	?	D	11.809
17	[ ] UO2.86!1.5H2O - Uranium Oxide Hydrate	49.9	10	0.000	1.000	23-1461	?	V	5.590

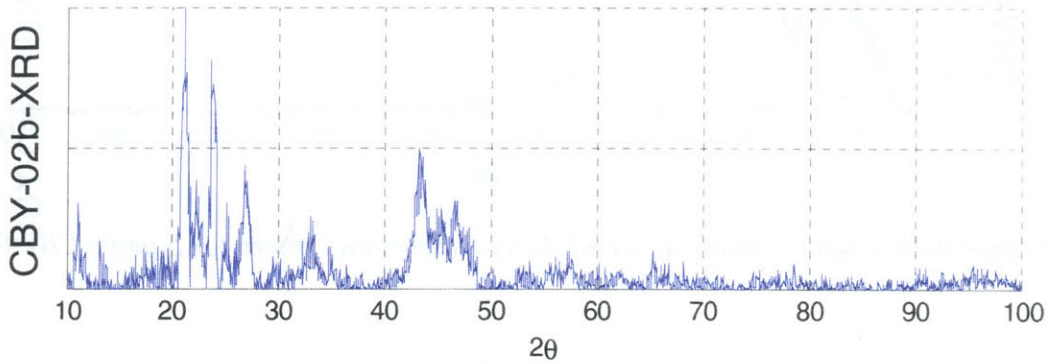

Figure B.9 – *Search Match List and X-ray Diffraction Pattern for Sample CBY-02b*: This sample was removed from the bed.

[Z14580.RAW] CBY-03 | S/M Hit Listing

SCAN: 10.0/100.0/0.05/1.75(sec), Cu, I(max)=1990, 07/11/03 15:29

NOTE: Intensity = Counts, 2T(0)=0.0(°), S/M: Default Search_Match (Use Chemistry Filter)

J-Column: [+] Common/Good Patterns, [?] Uncommon/Non-Ambient Patterns, [ ] Intermediate Patterns, [D] Deleted

D-Column: C=Calculated, D=Diffractometer, F=Densitometer, V=Film/Visual, X=Other/Unknown

#	40 Hits Sorted on Figure-Of-Merit	FOM	I%	2T(0)	d/d(0)	PDF-#	J	D	Density
1	Corundum, syn - Al2O3	12.1	34	-0.060	1.000	10-0173	+	D	4.050
2	UF4 - Uranium Fluoride	14.6	88	-0.060	1.000	32-1401	?	D	0.560
3	Diaspore - AlO(OH)	28.5	47	0.000	1.000	05-0355	+	D	3.440
4	Al2O3 - Aluminum Oxide	32.3	31	0.060	1.000	50-1496	+	X	3.397
5	Unnamed mineral [NR] - UO3·H2O	35.7	14	-0.060	1.000	15-0569	?	X	
6	Ianthinite - U6O7(OH)20	38.2	7	0.060	1.000	12-0272	?	V	5.160
7	H2U3O10 - Hydrogen Uranium Oxide	42.3	86	0.000	1.000	27-0201	?	C	6.851
8	UO3·H2O - Uranium Oxide Hydrate	42.8	31	0.060	1.000	11-0325	?	V	
9	UO2(OH)2 - Uranyl Hydroxide	44.9	9	-0.060	1.000	30-1403	?	X	5.820

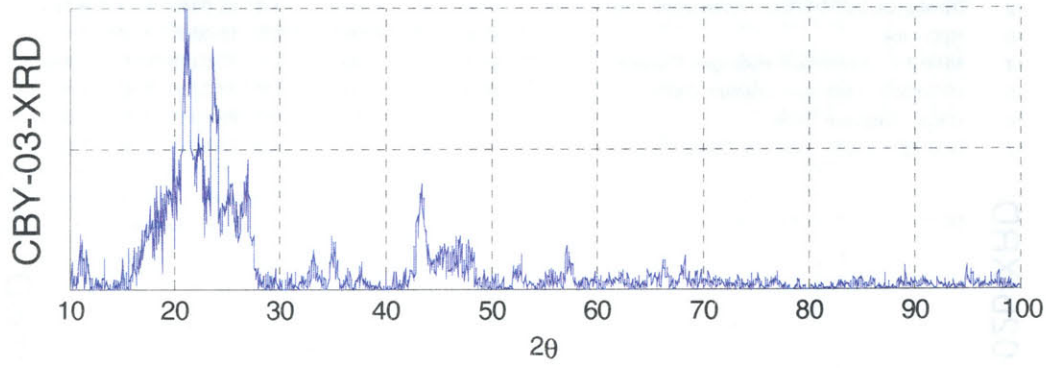

Figure B.10 – *Search Match List and X-ray Diffraction Pattern for Sample CBY-03*

[Z14759.RAW] CBY-04 S/M Hit Listing

SCAN: 10.0/100.0/0.05/1.75(sec), Cu, I(max)=3290, 07/23/03 22:40

NOTE: Intensity = Counts, 2T(0)=0.0(°), S/M: Default Search_Match (Use Chemistry Filter)

J-Column: [+] Common/Good Patterns, [?] Uncommon/Non-Ambient Patterns, [ ] Intermediate Pat...

D-Column: C=Calculated, D=Diffractometer, F=Densitometer, V=Film/Visual, X=Other/Unknown

#	40 Hits Sorted on Figure-Of-Merit	FOM	I%	2T(0)	d/d(0)	PDF-#	J	D
1	Corundum, syn - Al2O3	3.0	50	0.000	1.000	46-1212	+	D
2	AlF3 - Aluminum Fluoride	22.1	25	-0.060	1.000	44-0231	+	D
3	Al5O6N - Aluminum Oxide Nitride	24.9	33	0.120	1.000	48-0686	+	D
4	Al6O3N4 - Aluminum Oxide Nitride	28.1	12	0.060	1.000	48-1579	+	V
5	Al9O3N7 - Aluminum Oxide Nitride	28.6	33	0.120	1.000	48-1582	+	V
6	Al7O3N5 - Aluminum Oxide Nitride	35.7	12	0.000	1.000	48-1580	+	V
7	Al2O3 - Aluminum Oxide	39.2	15	0.000	1.000	50-0741	+	V
8	U3O8 - Uranium Oxide	39.7	33	0.000	1.000	43-1419	?	V
9	Al196O288N4 - Aluminum Oxide Nitride	41.6	18	0.060	1.000	20-0043		X
10	U2N3 - Uranium Nitride	45.2	17	0.000	1.000	15-0426	?	D
11	UN2 - Uranium Nitride	46.1	20	0.060	1.000	65-2973	?	C
12	(NH4)2UF6 - Ammonium Uranium Fluoride	48.0	23	0.000	1.000	16-0750	?	V

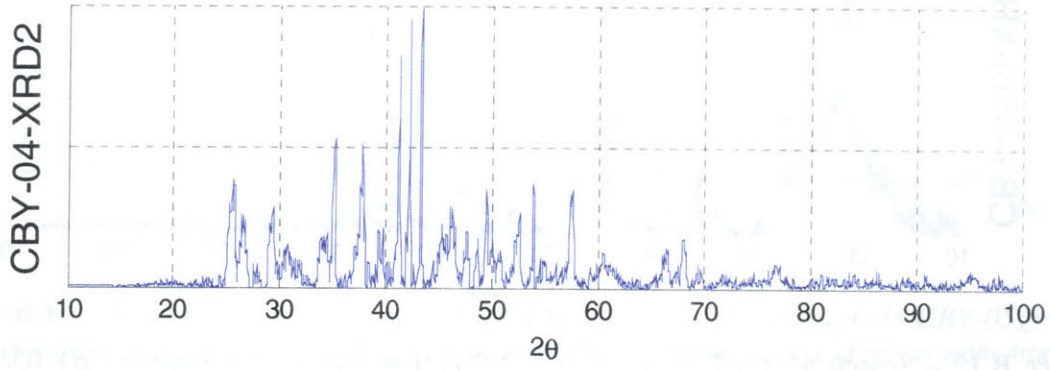

Figure B.11 – Search *Match List and X-ray Diffraction Pattern for Sample CBY-04*

[Z14582.RAW] CBY-05BL S/M Hit Listing

SCAN: 10.0/100.0/0.05/1.75(sec), Cu, I(max)=2005, 07/11/03 15:45

NOTE: Intensity = Counts, 2T(0)=0.0(°), S/M: Default Search_Match (Use Chemistry Filter)

J-Column: [+] Common/Good Patterns, [?] Uncommon/Non-Ambient Patterns, [ ] Intermediate Patterns, [D] Deleted

D-Column: C=Calculated, D=Diffractometer, F=Densitometer, V=Film/Visual, X=Other/Unknown

#	40 Hits Sorted on Figure-Of-Merit	FOM	I%	2T(0)	d/d(0)	PDF-#	J	D	Density
1	UF4 - Uranium Fluoride	15.5	86	0.060	1.000	32-1401	?	D	6.560
2	Corundum, syn - Al2O3	23.4	31	0.000	1.000	10-0173	+	D	4.050
3	Diaspore - AlO(OH)	24.3	46	-0.120	1.000	05-0355	+	D	3.440
4	Al2O3 - Aluminum Oxide	29.6	40	-0.060	1.000	50-1496	+	X	3.397
5	H2O - Ice	38.2	41	-0.120	1.000	42-1141	?	C	0.917
6	H2U3O10 - Hydrogen Uranium Oxide	40.0	85	0.060	1.000	27-0201	?	C	6.851
7	AlF3 - Aluminum Fluoride	44.4	5	0.060	1.000	43-0435	+	V	2.815
8	UO3 - Uranium Oxide	45.5	69	-0.120	1.000	18-1429	?	V	8.540
9	N5H5 - Hydrazine Azide	46.7	28	-0.060	1.000	26-0751	+	V	1.400
10	UOF4 - Uranium Oxide Fluoride	48.8	43	0.060	1.000	31-1429	?	V	5.700
11	UO3!H2O - Uranium Oxide Hydrate	49.6	31	0.060	1.000	11-0325	?	V	

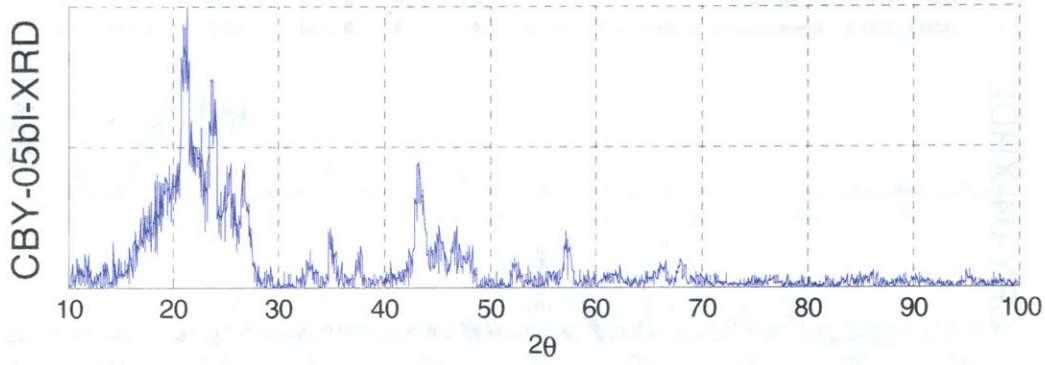

Figure B.12 – Search *Match List and X-ray Diffraction Pattern for Sample CBY-05bl*: This sample was selectively picked from CBY-05 to try to get a majority of the black powder from the sample while avoiding the green powder.

[Z14581.RAW] CBY-05GR | S/M Hit Listing

SCAN: 10.0/100.0/0.05/1.75(sec), Cu, I(max)=1747, 07/11/03 15:37

NOTE: Intensity = Counts, 2T(0)=0.0(°), S/M: Default Search_Match (Use Chemistry Filter)

J-Column: [+] Common/Good Patterns, [?] Uncommon/Non-Ambient Patterns, [ ] Intermediate Patterns, [D] Deleted

D-Column: C=Calculated, D=Diffractometer, F=Densitometer, V=Film/Visual, X=Other/Unknown

#	40 Hits Sorted on Figure-Of-Merit	FOM	I%	2T(0)	d/d(0)	PDF-#	J	D	Density
1	UF4 - Uranium Fluoride	9.9	86	-0.060	1.000	32-1401	?	D	6.560
2	Unnamed mineral [NR] - UO3-H2O	30.6	20	0.000	1.000	15-0569	?	X	
3	(NH4)2(UO2)2F5I3H2O - Ammonium Uranyl Fluor...	34.4	18	0.000	1.000	25-0046	?	D	4.280
4	Diaspore - AlO(OH)	40.1	31	-0.060	1.000	05-0355	+	D	3.440
5	Ianthinite - U6O7(OH)20	41.4	7	0.000	1.000	12-0272	?	V	5.160
6	UO2F2-x(OH)xI2H2O - Uranyl Fluoride Hydroxide ...	47.4	10	0.000	1.000	28-1411	?	D	3.800
7	Corundum, syn - Al2O3	48.0	36	0.060	1.000	10-0173	+	D	4.050

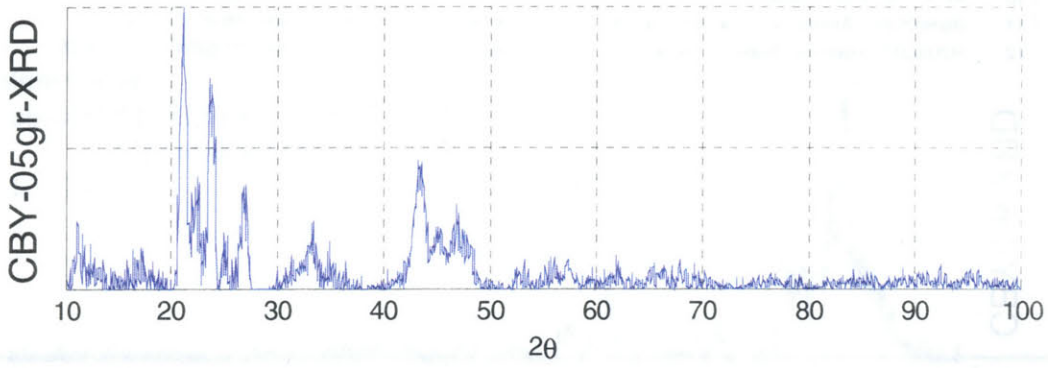

Figure B.13 – Search *Match List and X-ray Diffraction Pattern for Sample CBY-05gr*: This sample was selectively picked from CBY-05 to try to get a majority of the green powder from the sample while avoiding the black powder.

[Z14584.RAW] CBY-06 — S/M Hit Listing

SCAN: 10.0/100.0/0.05/1.75(sec), Cu, I(max)=1971, 07/11/03 16:58

NOTE: Intensity = Counts, 2T(0)=0.0(°), S/M: Default Search_Match (Use Chemistry Filter)

J-Column: [+] Common/Good Patterns, [?] Uncommon/Non-Ambient Patterns, [ ] Intermediate Patterns, [D] Deleted

D-Column: C=Calculated, D=Diffractometer, F=Densitometer, V=Film/Visual, X=Other/Unknown

#	40 Hits Sorted on Figure-Of-Merit	FOM	I%	2T(0)	d/d(0)	PDF-#	J	D	Density
1	✓ UF4 - Uranium Fluoride	16.8	94	0.060	1.000	32-1401	?	D	6.560
2	✓ Corundum, syn - Al2O3	17.2	21	0.000	1.000	10-0173	+	D	4.050
3	Diaspore - AlO(OH)	25.0	50	-0.060	1.000	05-0355	+	D	3.440
4	✓ Uraninite, syn - UO2	36.3	21	-0.060	1.000	65-0285	?	C	10.953
5	N5H5 - Hydrazine Azide	40.5	36	-0.060	1.000	26-0751	+	V	1.400
6	Uraninite-Q, syn - U3O7	42.7	20	-0.060	1.000	15-0004	?	V	11.316
7	UO3H2O - Uranium Oxide Hydrate	43.0	20	0.000	1.000	18-1437	?	D	5.560
8	Al2O3 - Aluminum Oxide	44.0	25	0.060	1.000	50-1496	+	X	3.397
9	✓ UO3 - Uranium Oxide	44.2	70	-0.120	1.000	45-0857	?	V	8.548
10	AlF3 - Aluminum Fluoride	45.0	7	0.060	1.000	43-0435	+	V	2.815
11	(NH4)2UF6 - Ammonium Uranium Fluoride	47.4	7	0.060	1.000	16-0750	?	V	
12	H2U3O10 - Hydrogen Uranium Oxide	49.8	88	0.120	1.000	27-0201	?	C	6.851

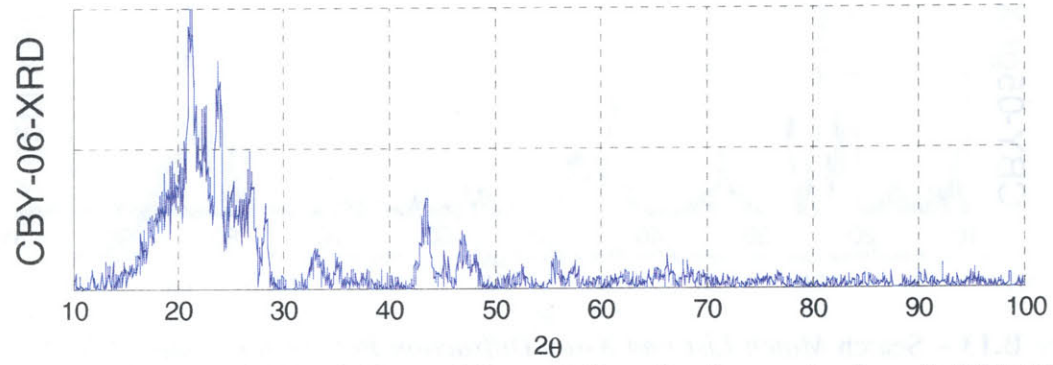

Figure B.14 – Search *Match List and X-ray Diffraction Pattern for Sample CBY-06*

Appendix C ICP-AES Data

C-1 Total Uranium

sample	uranium concentration g/L	uranium concentration mol/L	background (cps) μ ± σ	gross rate (cps) μ ± σ	net rate (cps) μ ± σ
std_0.005*	0.005	2.10E-05	22231 78.0	31144 10.33	8913 78.68
std_0.01	0.01	4.20E-05	22375 203.1	73373 319.8	50998 378.8
std_0.01-end†	0.01	4.20E-05	22314 216.6	72904 314.6	50590 382
std_0.02	0.02	8.40E-05	22335 190.1	105805 955	83470 973.7
std_0.02-end†	0.02	8.40E-05	22275 60.9	104817 1022	82542 1024
std_0.05	0.05	2.10E-04	22187 174.4	278156 1620	255969 1629
std_0.05-end†	0.05	2.10E-04	22433 169.1	277140 2760	254707 2765
std_0.1*	0.1	4.20E-04	22262 156.9	442737 2301	420475 2306

* not used in calibration since these points fell well outside expected concentration values
† these standards were run after the unknown samples to check calibration

Table C.1 – Calibration Standard Data for Total Uranium Dissolution Analysis

Calibration Curve

cps=[U]*1251840052-10532

[U] [=] mol U/L

R^2=99.09%

sample ICP-AES #	sample ID	background μ ± σ	gross counts μ ± σ	net counts μ ± σ	uranium concentration g/L
1d-2	CBY-lggcol-1	22453 63.8	105185 629	82732 632.2	0.0177 ± 0.0026
2d-2	CBY-bm-2	22257 137.2	97628 249	75371 284.6	0.0163 ± 0.0023
3d-2	CBY-01	22241 60.6	151928 1485	129687 1486	0.0267 ± 0.0038
4d-2	CBY-02a	22242 225.2	149723 708	127481 743	0.0262 ± 0.0038
5d-2	CBY-02b	22254 221.2	183847 840	161593 868.6	0.0327 ± 0.0047
6d-2	CBY-03	22060 63.5	147393 495	125333 499.3	0.0258 ± 0.0037
7d-2	CBY-05	22046 107.2	153311 272	131265 292.5	0.0270 ± 0.0039
8d-2	CBY-06	22216 165.3	145553 802	123337 818.9	0.0255 ± 0.0037
9d-2	CBY-04	22335 74.7	160095 1882	137760 1883	0.0282 ± 0.0041
10d-2	UO_2	22415 209.8	245636 2777	223221 2785	0.0444 ± 0.0064
11x-3	UF_4	22511 56.9	74618 571	52107 573.8	0.0119 ± 0.0017

Table C.2 – Unknown Sample Data for Total Uranium Dissolution Analysis

C-2 Water Soluble Uranium

sample	[U]	background (cps)			gross rate (cps)			net rate (cps)		
	g/L	μ	±	σ	μ	±	σ	μ	±	σ
std_0.5	0.5	22906	±	474	1706000	±	14034	1683094	±	14042
std_0.1	0.1	22672	±	433.5	459118	±	4154	436446	±	4176.558
std_0.05	0.05	21557	±	1401	270049	±	1401	248492	±	1981.313
st_0.005	0.005	21542	±	67.8	29962	±	87.9	8420	±	111.0101

Table C.3 – Calibration Standard Data for Water-Soluble Uranium Dissolution Analysis

The calibration curve was done by linear interpolation between bracketing points.

for values between 0.1 and 0.5 g/L
slope: 3116620
intercept: 124784

for values between 0.05 and 0.1 g/L
slope: 3759080
intercept: 60538

for values between 0.005 and 0.05 g/L
slope: 5334933
intercept: -18254.7

sample		background (cps)			gross cpm			net cpm			[U] g/L
2f	CBY-bm-2	20766	±	80.2	426392	±	4186	405626	±	4187	0.0918
3f	CBY-01	21425	±	129.6	439653	±	1998	418228	±	2002	0.0952
4f	CBY-02a	23205	±	133.8	1306000	±	18593	1282795	±	18593	0.3716
5f	CBY-02b	22276	±	93.7	719307	±	10129	697031	±	10129	0.1836
6f	CBY-03	22421	±	712	1109900	±	4343	1087479	±	4401	0.3089
7f	CBY-05	21344	±	48.67	1271000	±	11054	1249656	±	11054	0.3609
8f	CBY-06	21570	±	147.2	846461	±	6474	824891	±	6476	0.2246
9f	CBY-04	21511	±	59.9	669818	±	7455	648307	±	7455	0.1680
10f	UO_2	21411	±	150.9	41024	±	572	19613	±	592	0.0071
11f-1	UF_4	21636	±	11.03	457836	±	6749	436200	±	6749	0.0999
11f-2*	UF_4	21629	±	107.8	447726	±	565	426097	±	575	0.0972

Table C.4 – Unknown Sample Data for Water-Soluble Uranium Dissolution Analysis

Appendix D Heating Cycles

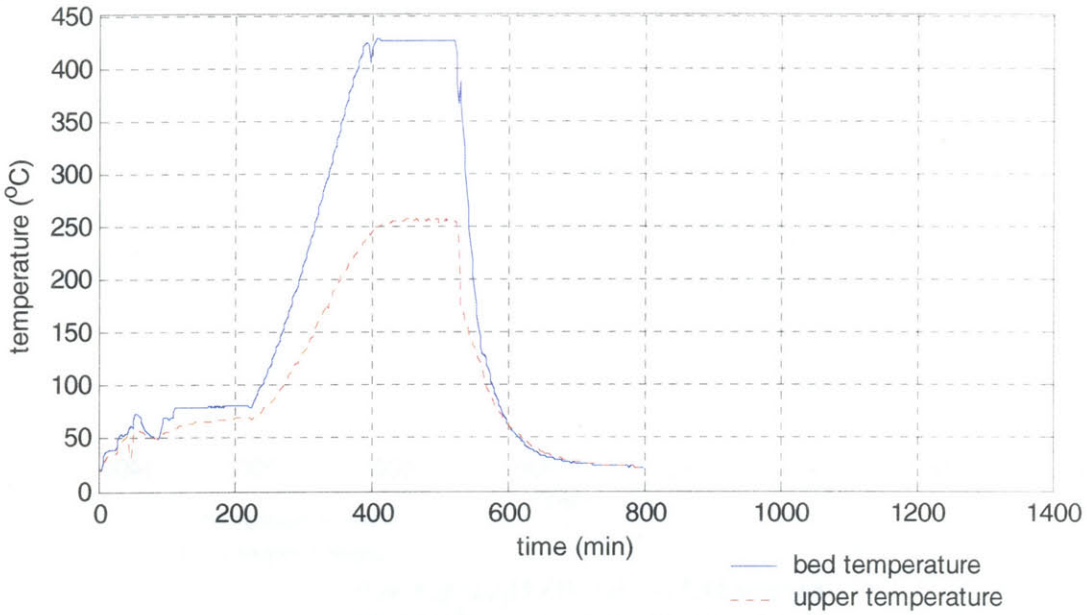

Figure D.1 – CBY-01 Heating Cycle

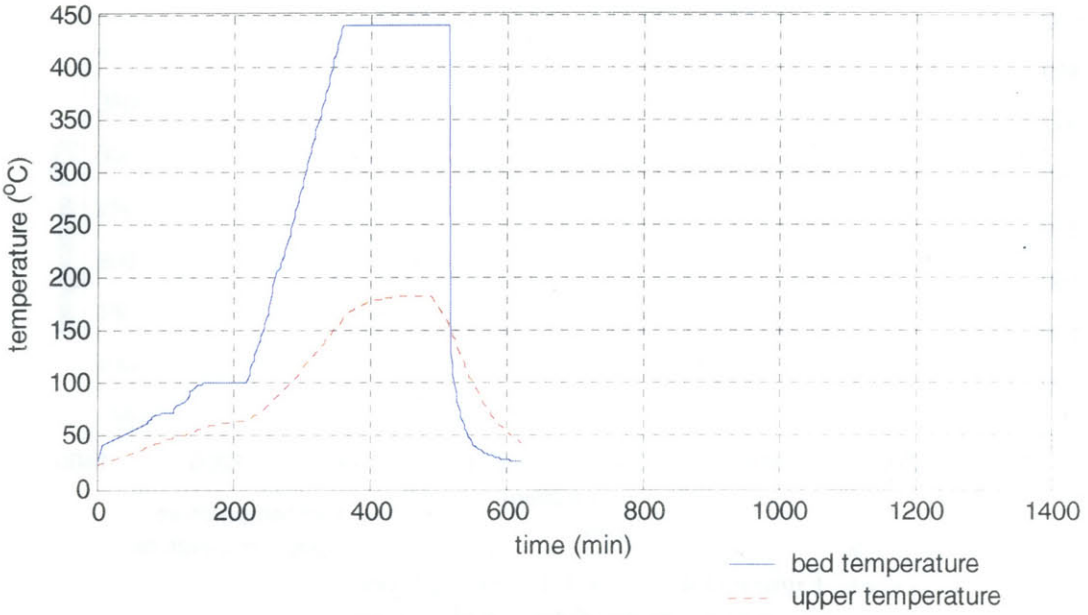

Figure D.2 – CBY-02 Heating Cycle

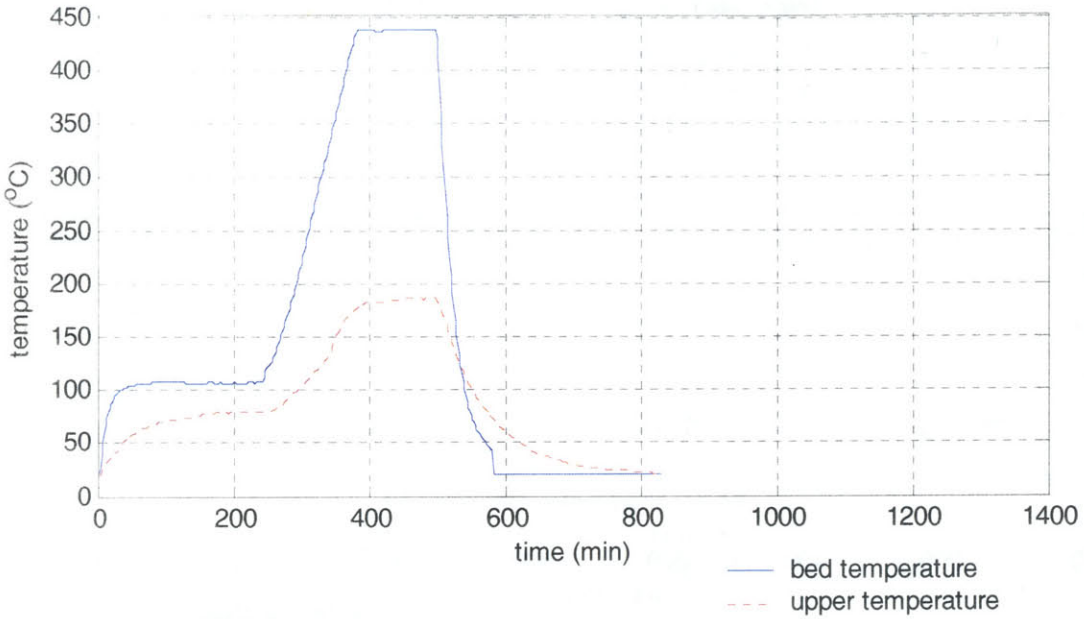

Figure D.3 – CBY-03 Heating Cycle

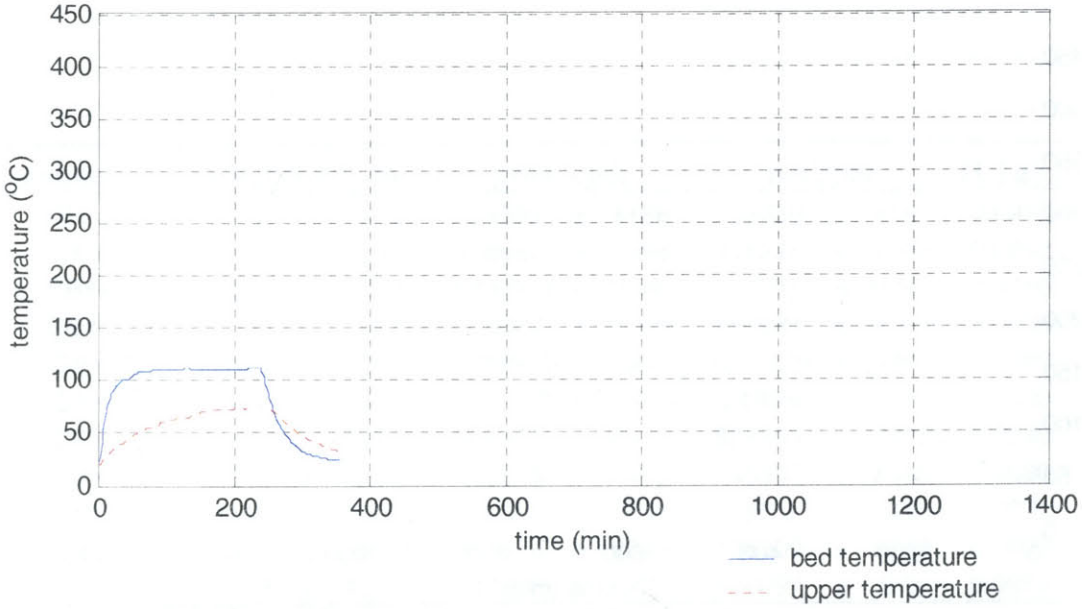

Figure D.4 – CBY-04 Heating Cycle

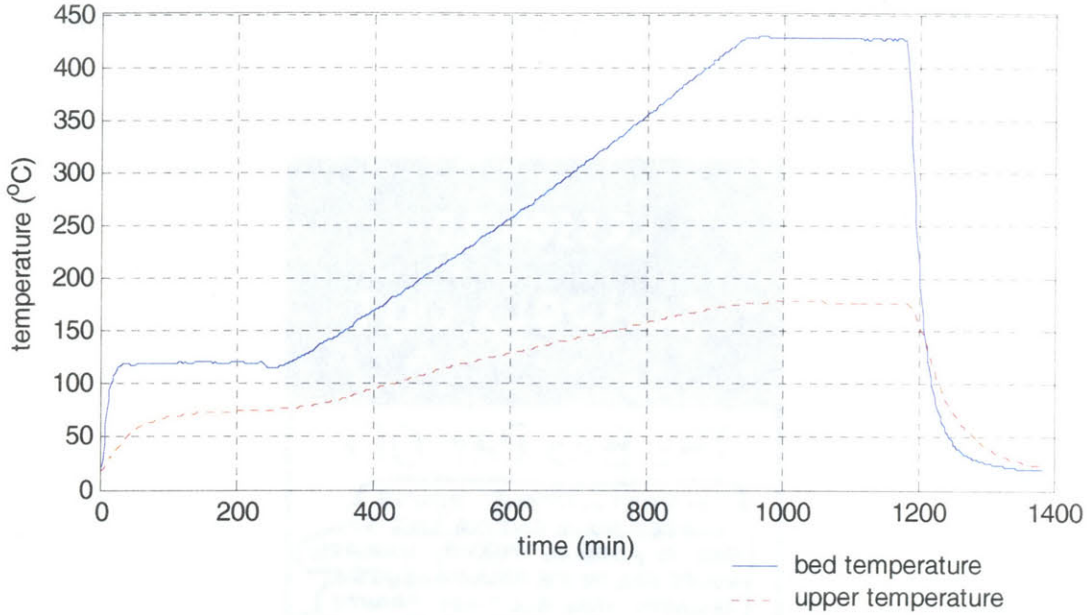

Figure D.5 – CBY-05 Heating Cycle

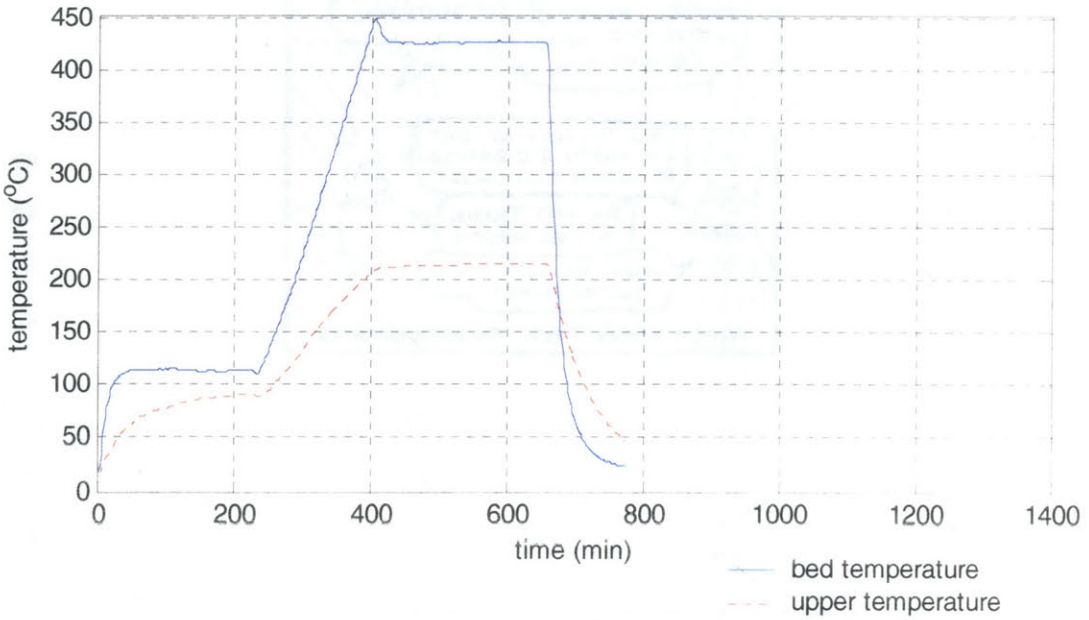

Figure D.6 – CBY-06 Heating Cycle

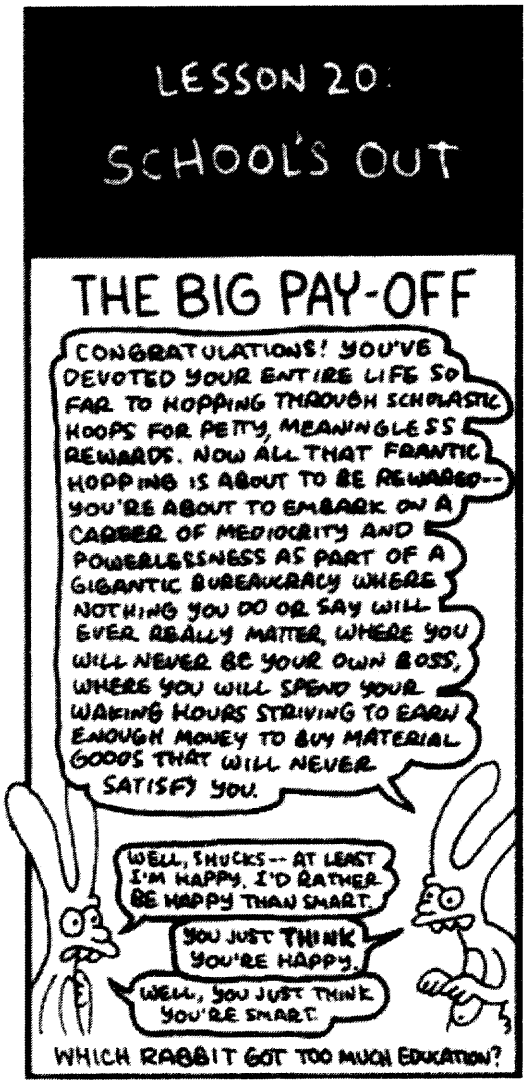
LESSON 20:
SCHOOL'S OUT
THE BIG PAY-OFF
CONGRATULATIONS! YOU'VE DEVOTED YOUR ENTIRE LIFE SO FAR TO HOPPING THROUGH SCHOLASTIC HOOPS FOR PETTY, MEANINGLESS REWARDS. NOW ALL THAT FRANTIC HOPPING IS ABOUT TO BE REWARDED-- YOU'RE ABOUT TO EMBARK ON A CAREER OF MEDIOCRITY AND POWERLESSNESS AS PART OF A GIGANTIC BUREAUCRACY WHERE NOTHING YOU DO OR SAY WILL EVER REALLY MATTER, WHERE YOU WILL NEVER BE YOUR OWN BOSS, WHERE YOU WILL SPEND YOUR WAKING HOURS STRIVING TO EARN ENOUGH MONEY TO BUY MATERIAL GOODS THAT WILL NEVER SATISFY YOU.
WELL, SHUCKS -- AT LEAST I'M HAPPY. I'D RATHER BE HAPPY THAN SMART.
YOU JUST THINK YOU'RE HAPPY.
WELL, YOU JUST THINK YOU'RE SMART.
WHICH RABBIT GOT TOO MUCH EDUCATION?

Appendix E Carrier Gas Flow Data

Gas flow was measured with a Bel-Art Riteflow® 150mm size 4 flowmeter (part number H40407-0215). Values given are the flowmeter reading for the stainless steel float.

sample	gas flow
CBY-01	100
CBY-02	30
CBY-03	20
CBY-04	20
CBY-05	20
CBY-06	15

Table E.1 – Carrier Gas Flow Values

flowmeter reading stainless float	air flow mL/min
150	17430
140	16287
130	16194
120	14057
110	12944
100	11814
90	10607
80	9462
70	8307
60	7156
50	5977
40	4732
30	3464
20	2225
10	959

Table E.2 – Calibration of Flowmeter for Air at 1 atm, 70 °F

THIS PAGE INTENTIONALLY LEFT BLANK

Appendix F – Sample Masses and Run Yields

Sample CBY-lggcol-01 was used as feedstock for all fluidized bed samples except CBY-01. CBY-01 used CBY-lggcol-4, which had not been ball milled, as feedstock.

Composition of sample CBY-lggcol-01:

19.8940 g UO_2

17.6848 g NH_4HF_2

➔ 2.37 weight percent excess NH_4HF_2

Table F.1 – Masses and Yields of Fluidized Bed Samples

sample	initial mass	theoretical UF_4 yield	actual final mass	gross yield
	g	g	g	
CBY-01	2.8042	1.7248	1.2749	73.9%
CBY-02*	2.7958	1.7196	1.3508	78.6%
CBY-03	2.857	1.7573	1.5275	86.9%
CBY-04†	2.8018	2.3333	2.3036	98.7%
CBY-05	2.8218	1.7356	1.6982	97.8%
CBY-06	2.814	1.7308	1.72282	99.5%

* Since the high argon flow rate carried a large amount of the sample onto the top flange of the column, the number given here is the sum of both samples CBY-02a (top flange) and CBY-02b (bed).

† This sample was an attempt to decompose the sample to its intermediate product at 110 °C. Based on TGA analysis, the intermediate product appears to be $(NH_4)_3UF_7$, so this value was used instead of that for UF_4 in calculating theoretical yield.

THIS PAGE INTENTIONALLY LEFT BLANK

S993-92